Vulnerability assessment and feasibility analysis of seismic strengthening of school buildings

C.Z. Chrysostomou[1], N. Kyriakides[1], V.K. Papanikolaou[2] , A.J. Kappos[2,3], E.G. Dimitrakopoulos[4], A.I. Giouvanidis[4]

Abstract

The majority of structures in seismic-prone areas worldwide are structures that have been designed either without seismic design considerations, or using codes of practice that are seriously inadequate in the light of current seismic design principles. In Cyprus, after a series of earthquakes that occurred between 1995 and 1999, it was decided to carry out an unprecedented internationally seismic retrofitting of all school buildings, taking into account the sensitivity of the society towards these structures. In this paper representative school buildings are analysed in both their pristine condition and after applying retrofitting schemes typical of those implemented in the aforementioned large-scale strengthening programme. Non-linear analysis is conducted on calibrated analytical models of the selected buildings and fragility curves are derived for typical reinforced concrete and unreinforced masonry structures. These curves are then used to carry out a feasibility study, including both benefit-cost and life-cycle analysis, and evaluate the effectiveness of the strengthening programme.

Keywords: school buildings; seismic vulnerability assessment; non-linear dynamic analysis; cost-benefit analysis; life-cycle cost analysis.

1. Introduction

As noted in OECD (2004) "schools built world-wide routinely collapse in earthquakes due to avoidable errors in design and construction, because existing technology is not applied and existing laws and regulations are not sufficiently enforced". In fact the majority of schools in seismic-prone areas worldwide are structures that have been designed either without seismic design considerations, or using codes of practice that are seriously inadequate in the light of current seismic design principles. Given their particularly sensitive role in the society, schools are given high priority when earthquake strengthening programmes are discussed; nevertheless, due to economic constraints, a very small fraction of the existing school building stock has actually been upgraded in the frame of pre-earthquake strengthening programmes world-wide. Until recently, the most extensive efforts in implementing school strengthening programmes were made in Japan; some interesting examples of such applications are given in Japan

---

[1] Department of Civil Engineering and Geomatics, Cyprus University of Technology, Limassol, Cyprus

[2] Department of Civil Engineering, Aristotle University of Thessaloniki, Greece

[3] Department of Civil Engineering, City University London, UK; e-mail: Andreas.Kappos.1@city.ac.uk

[4] Department of Civil and Environmental Engineering, Hong Kong University of Science & Technology

Ministry of Education (2006). However, overall, the number of strengthened buildings is very low, compared to the entire stock. Moreover, recent efforts towards setting up large-scale strengthening (also referred to as retrofit) programmes of school buildings, such as that in British Columbia (Ventura et al. 2012) are useful in that they introduce concepts like performance based assessment and compilation of web-based databases of results of advanced analysis of such buildings, but, to the authors' best knowledge, have not culminated into actual implementation of strengthening schemes to even a limited number of schools. In this respect, the case of Cyprus, discussed in this paper, is a particularly notable one, since it practically covered the entirety of the school building stock in the country.

Historical reports and archaeological findings in Cyprus show that in the period from 1896 to 2004 more than 400 earthquakes occurred, 5 of which were of magnitude higher than 5.6 and have caused limited fatalities but severe damage to the building stock. Despite the recorded history of destructive earthquakes, the first seismic design measures in Cyprus were imposed after 1986 and the first seismic design code was introduced on a voluntary basis in 1992 and was enforced in 1994. In 2012, all previous standards were withdrawn and were replaced by the Eurocodes. Therefore, the majority of structures, including schools, have been designed without any seismic provisions. The Cyprus State, has decided an unprecedented internationally seismic retrofitting of all deficient school buildings, primarily taking into account the sensitivity of the society towards these structures. The total number of school buildings in Cyprus is 660. Of these, 26 were demolished and replaced by new ones at a cost of about 31 million Euros and 280 were retrofitted at a cost of 140 million Euros. The rest were designed after the enforcement of the seismic codes and were found to not require any intervention. To date, about 90% of the school buildings of Cyprus are deemed to possess adequate seismic resistance (Chrysostomou et al. 2013).

The effectiveness of this programme was evaluated in a recent research project, and this paper reports all parts of the project that are of interest to an international audience. In the first part representative school buildings are analysed in both their pristine condition and after applying retrofitting schemes typical of those implemented in the aforementioned large-scale strengthening programme. The selection or the representative buildings is described in Chrysostomou et al. (2013) along with a detailed description of their characteristics. Non-linear analysis is conducted on calibrated analytical models of the selected buildings and fragility curves are derived for typical reinforced concrete (R/C) and unreinforced masonry (URM) structures. In the second part, a feasibility study is conducted, including both benefit-cost and life-cycle analysis, the effectiveness of the strengthening programme is evaluated and optimum retrofit levels are proposed for each building type examined. These can serve as a guide for any future strengthening programme of important buildings characterised by unacceptable level of earthquake risk.

2. Fragility curves for school buildings before and after retrofit

2.1. Reinforced concrete buildings

R/C buildings may exhibit inelastic non-linear behaviour when subjected to seismic loading, especially in the case of existing non-seismically designed ones, which are expected to experience such behaviour even at low intensity earthquakes and suffer severe damage. In the case of modern buildings designed to seismic codes, this non-linear behaviour can be sustained by the building for moderate to high earthquakes without exhibiting severe damage due to modern design and detailing practices. The non-linear behaviour of a building depends mainly on the quality and strength of materials and the detailing of its members and their connections.

In the case of school buildings in Cyprus the majority of them are low-rise R/C frames, having one direction considerably longer than the other and a skylight. To assess the performance of such buildings through life-cycle assessment, fragility curves were derived based on the limit states of Eurocode 8-Part 3 (CEN, 2005). A representative R/C school building was selected as the case study building and a

probabilistic methodology was used to derive simulation buildings to cover the wide range of uncertainties both in the capacity of these buildings and in the hazard excitation.

To derive the fragility curves detailed analytical simulation of its non-linear behaviour was established through the use of appropriate software. In this case, ANSRuop (http://www.strulab.civil.upatras.gr/software) was selected since it includes a fibre element for the simulation of beam and column elements, which accounts for the reduction in stiffness due to cracking, and provides information during the analysis regarding the attainment of the Eurocode 8-Part 3 limit states by the structural elements of the building. The plastic rotations and shear forces are calculated in every step of the analysis and are compared to the corresponding limit state capacities as defined in Eurocode 8-Part 3 (Annex A). The limit state corresponding to each element is graphically shown during the analysis which provides straightforward information regarding the state of the structure and the propagation of damage. Thus the probability of reaching or exceeding these limit states by the simulation frame was calculated from the results of the analysis and used to derive fragility curves for the limit states.

2.1.1 Description of the selected R/C school building

The selected R/C school building was approximately 200 m^2 in plan (20m×10m) with R/C frames at 3m spacing providing the resistance in the short direction. In the long direction two lines of columns are present connected only through the slab (no beams). A skylight extending to a height of approximately 500mm below the slab was left open to enhance the lighting of the building. During the retrofitting of the building steel truss members were introduced to strengthen the opening and provide frame action in the long direction as well. Columns are placed in two lines, one on each side of the building in the long direction. The initial dimensions of all columns were 300mm×300mm. More than half of them were increased in area (500mm×500mm) using R/C jackets for retrofitting purposes. A view of the selected building is given in Figure 1 whereas a plan of the building with the retrofitted columns shown in dark hatch is given in Figure 2.

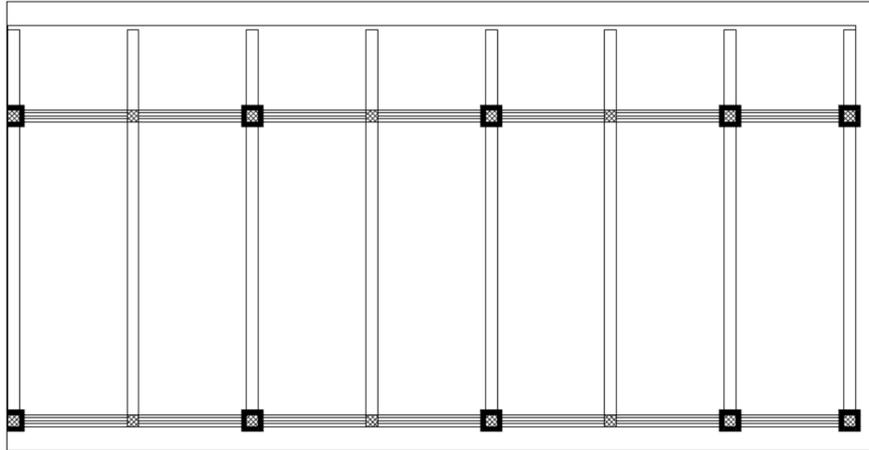Figure 1. Front elevation of the R/C school-building

Figure 2. Plan of the R/C school-building

2.1.2 Modelling of the building

The analytical simulation of the selected building was conducted on ANSRuop, a non-linear analysis academic software geared towards the assessment of R/C buildings based on Eurocode 8-Part 3. Both columns and beams (frame elements) were modelled using line elements whereas slabs were modelled using plate elements and were assumed to remain linear elastic.

Initially the strengthened building was modelled using the elastic properties of materials to obtain its analytical fundamental frequency. Reduced flexural rigidity (EI_{eff}) was assumed equal to 50% of the uncracked value of the sections as prescribed in Eurocode 8 (CEN, 2004b) for R/C members. In the nonlinear analysis EI_{eff} was calculated from the moment vs curvature relationship (Figure 3), as suggested by Eurocode 8 – Part 3 (CEN 2005); curvature is calculated from the yield rotation given in the code (i.e. $EI_{eff}=M_yL_v/3\theta_y$, where L_v is the shear span). At the same time, in situ measurements were conducted using an accelerometer network to obtain the dynamic properties of the strengthened building. Details on the procedure followed for the recordings and the results of the processing of the measurements can be found in Chrysostomou et al. (2013).

The analytically derived fundamental mode shape of the building (natural period 0.79 sec) in the X direction is shown in Figure 4. The effective modal mass of the 1st mode is 70%. The 2nd mode period, which corresponds to the 1st translational mode in the Y direction, was calculated to be 0.69 sec with an effective modal mass of 67%. The corresponding in-situ recordings showed very close correlation (0.78 and 0.67sec, respectively) to the analytical ones, which provided confidence to the elastic properties of the analytical model.

After establishing the accuracy of the elastic model of the strengthened building, the model was extended to account for the inelastic behaviour. For the non-strengthened elements concrete strength of $f_{cm}=24MPa$ was assumed (C16/20), whereas for columns with jacketing a mean concrete strength of $f_{cm}=33MPa$ corresponding to Eurocode 2 (CEN 2004a) concrete class C25/30 was adopted. Similarly, mean reinforcement yield strength of $f_{ym}=410MPa$ and 500MPa was adopted, for the existing and the strengthened members, respectively. The material strength classes were adopted based on the code design practice of the period of construction and strengthening of the building.

Frame elements were modelled using inelastic laws for concrete and steel and were discretized into concrete and steel fibres. The fibre element was used to generate their non-linear moment-curvature relationships based on the calculated axial loads. The jackets were modelled using also cracked stiffness (for nonlinear analysis) and were assumed as a uniform section. An example of the derived moment-curvature relationships for the fibre cross-section modelling of a column is given in Figure 3.
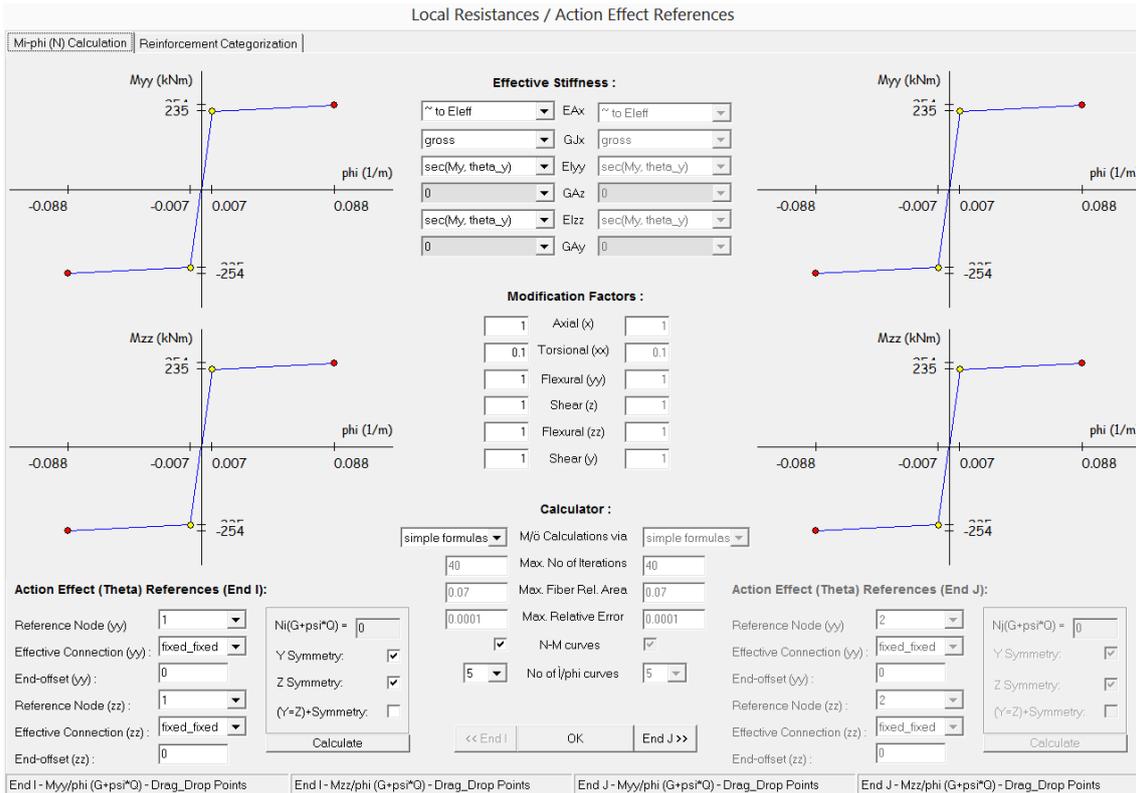
Figure 3. Moment-curvature relationships for strengthened columns
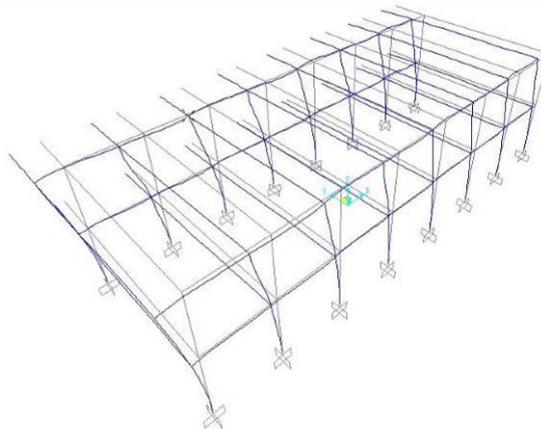
Figure 4. Structural model and fundamental mode shape of R/C building

2.1.3 Derivation of fragility curves

To assess the performance of the building based on the Eurocodes, it was decided to produce fragility curves based on the limit states defined in Eurocode 8-Part 3 (Annex A). This part of Eurocode 8 includes the limit states for the assessment of existing R/C buildings as well as mathematical models for the design of structural interventions. The three limit states included in Eurocode 8-Part 3 (CEN, 2005) for assessment purposes of existing R/C buildings are:

(1) Damage Limitation (DL): corresponding to yield rotational capacity.

(2) Significant Damage (SD): ¾ of the ultimate rotational capacity.

(3) Near Collapse (NC): corresponding to ultimate rotational capacity and/or shear capacity as defined in the code.

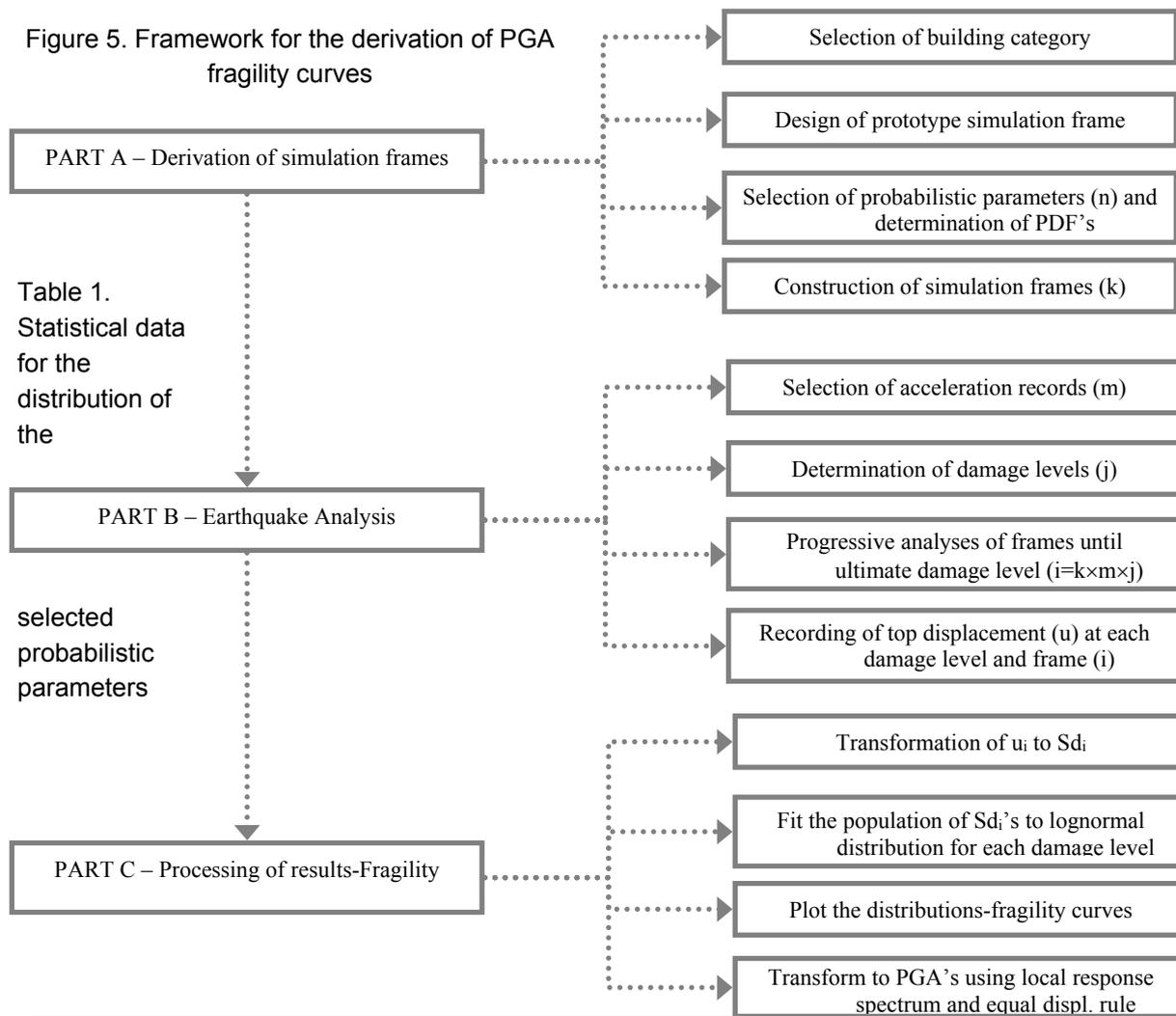For uniform treatment of the structures addressed in the present study, and in order to produce fragility curves that also include the probability of collapse of the building, a fourth limit state was also considered for the collapse of the building which was assumed to take place if 50% or more of the columns of a floor reached limit state 3 or a maximum inter-storey drift of 4% was reached. This collapse criterion is consistent with the one proposed by Kappos et al. (2006) as part of a hybrid method for vulnerability assessment of R/C and URM buildings.

Further to the definition of limit states, the procedure followed for the derivation of the fragility curves for the R/C school building is probabilistic both as far as the capacity of the building and the earthquake demand, are concerned. The framework for the derivation of the curves is divided into 3 parts and an outline of each part is given in Figure 5. Detailed discussion for each part is provided in the remainder of this section.

A number of simulation buildings were derived to account for the uncertainty in capacity whereas the uncertainty in demand was accounted for through the use of a number of peak ground acceleration (PGA) history records.

As far as the capacity of the building is concerned, four parameters were treated probabilistically based on the capacity models for the various credible failure modes. These consist of the strength of materials f_{cm} and f_y, the spacing of the shear reinforcement (s) and the development length (ℓ) of column bars. The strength of materials is correlated mainly to the flexural and shear capacity of the members, whereas the spacing and development length are correlated to their shear and bond capacities, respectively. The average values for all the parameters were obtained based on the design codes and practice at the period of construction of the building. The corresponding standard deviation values of the distribution of each parameter were obtained on the basis of the literature as described in Kyriakides (2014). Table 1 shows the values describing the probability distribution function (PDF) of each parameter. A normal distribution is assumed as the PDF for all parameters except f_y, which is assumed to follow a log-normal distribution. The values for non-seismic design shown in the Table were used for all members of the building that were not retrofitted, whereas the full seismic design was used for the modelling of the jackets. All other design parameters such as member dimensions, bar diameters etc., were treated deterministically as obtained from the structural drawings of the building.

Figure 5. Framework for the derivation of PGA fragility curves

PART A – Derivation of simulation frames

Table 1. Statistical data for the distribution of the

selected probabilistic parameters

PART B – Earthquake Analysis

PART C – Processing of results-Fragility

Selection of building category

Design of prototype simulation frame

Selection of probabilistic parameters (n) and determination of PDF's

Construction of simulation frames (k)

Selection of acceleration records (m)

Determination of damage levels (j)

Progressive analyses of frames until ultimate damage level (i=k×m×j)

Recording of top displacement (u) at each damage level and frame (i)

Transformation of u_i to Sd_i

Fit the population of Sd_i's to lognormal distribution for each damage level

Plot the distributions-fragility curves

Transform to PGA's using local response spectrum and equal displ. rule

Probabilistic Parameter	No seismic design		Full seismic design	
	Average	St.Deviation	Average	St.Deviation
f_{cm} (MPa)	24	8	33	6
f_y (MPa)	410	32	500	32
s (mm)	200	40	125	25
ℓ	30Φ	6Φ	40Φ	6Φ

In order to account for the uncertainty in these parameters a Latin Hypercube Sampling algorithm was used to derive a number of simulation buildings based on the distribution of the parameters. This technique, proposed by McKay (1979), enables the reduction in the number of simulations compared to the Monte Carlo technique (Ayyub and McCuen1995) by adopting a stratified approach in selecting the simulation values from the PDF. In order to determine the number of required simulation buildings to expedite convergence of the results, the 2n factorial composite method is used which prescribes (2n+2n+1) parameter combinations in order to account fully for the uncertainty associated with n independent random variables. Thus 25 simulation values from each PDF were generated using the above mentioned technique and were used to generate 25 corresponding simulation buildings based on the selected R/C strengthened school building. In order to assess the effect of strengthening and compare to the pristine R/C school building, the same number of simulation buildings were generated based on the no-seismic design PDF's of the four parameters for the original building without the column strengthening.

After the generation of the simulations of the pristine and strengthened R/C school buildings, the selection of appropriate acceleration records representing the seismic hazard in the area under consideration took place. The normalised acceleration response spectrum derived in the microzonation study for Limassol for the zone that the school is located was selected. This spectrum (Fig. 6) is the median spectrum at the location of the selected R/C school building and has a maximum amplification factor Ras = 2.5. The details of the study can be found in Anastasiades et al. (2006)
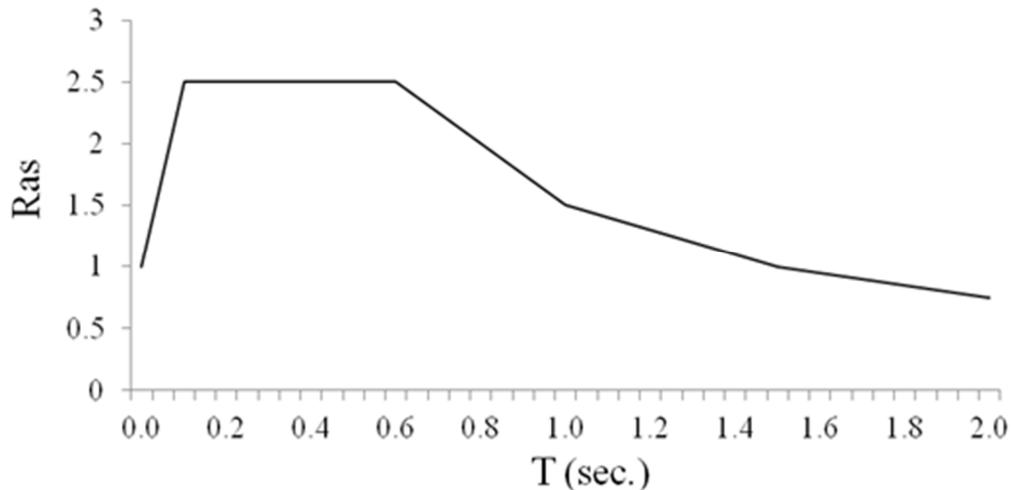

Figure 6. Normalised response spectrum based on the local microzonation study

Based on the above spectrum, and the form of the signals from 7 earthquakes in similar seismotectonic environments, 7 records were generated for the three directions of the earthquake. Each simulation building was analysed for each record, successively scaled until the collapse limit state was attained. The top storey displacement at each limit state was recorded and transformed to spectral displacement (S_d) by using the transformation to the equivalent single degree of freedom system for the fundamental mode shape of the structure.

Thus the mean S_d values and the corresponding standard deviation for all simulation buildings were obtained from the analysis results. By fitting these statistical values to a lognormal distribution the S_d fragility curves were created for each simulation model and damage level. These curves were derived in order to be applicable for use in the context of any capacity demand diagram method. Subsequently, the response spectrum for Limassol (Figure 6) was used along with the equal displacement rule to transform the mean S_d values into mean PGA ones. This transformation was deemed necessary in order to produce PGA-based fragility curves that can be used in the context of the selected life-cycle assessment. The approximations involved in this transformation can be regarded as acceptable when compared to the uncertainties and assumptions associated with the application of the life-cycle methodology.

In order to account for the additional uncertainty in the definition of the damage limit state an additional standard deviation β_{LS}=0.2 was assumed and was combined with the β-value calculated from the statistical processing of the results of the analytical simulations, using the square root of the sum of the squares. The β-value from the analysis was 0.3 for the strengthened school building and 0.35 for the school building in its pristine condition. These values include uncertainty associated with the demand and variability in capacity. The additional β-value used for the uncertainty in the definition of the damage limit state is half the one used in HAZUS (FEMA-NIBS 2003) since the limit states in Eurocode 8-Part 3 are assumed as well defined.

The statistical data of the PGA-based fragility curves for the R/C school buildings prior to, and after strengthening are given in Tables 2a and 2b. The corresponding fragility curves are given in Figures 7 and 8.

Table 2a. Fragility parameters for the R/C School building in its pristine condition

Limit State	Mean PGA (g)	Standard Deviation (β_{dsi})
DL	0.11	0.4
SD	0.19	0.4
NC	0.24	0.4
Collapse (Failure)	0.28	0.4

Table 2b. Fragility parameters for the strengthened R/C School building

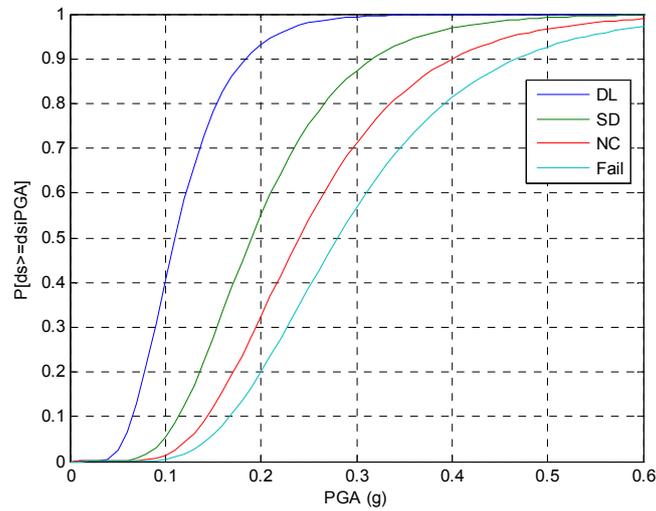| Limit State	Mean PGA (g)	Standard Deviation (β_{dsi})
DL	0.25	0.35
SD	0.50	0.35
NC	0.70	0.35
Collapse (Failure)	0.85	0.35

Figure 7. PGA fragility curves for the pristine R/C school building
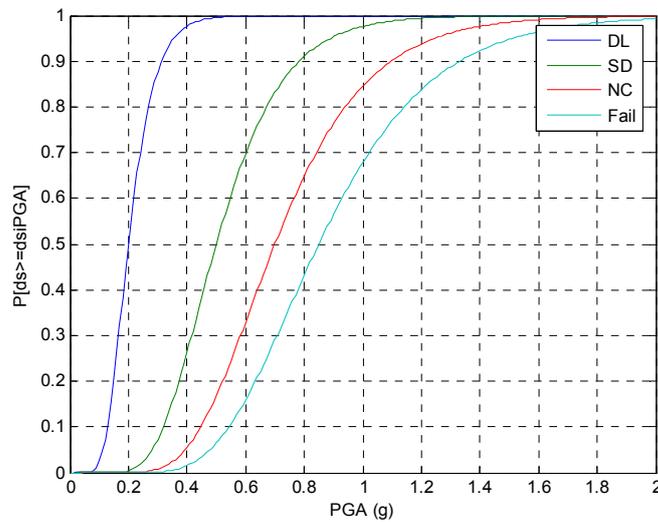

Figure 8. PGA fragility curves for the strengthened R/C school building

2.2. Masonry buildings

In the class of unreinforced masonry school buildings, the selected typical structure was a single-storey elementary school building located in Limassol; its plan dimensions are 34.75×22.10 m and total height is 7.30 m, consisting of load-bearing limestone masonry with the addition of a timber roof (Fig .9).
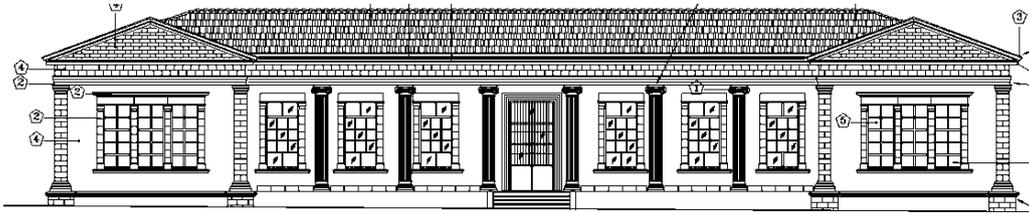

Fig. 9 Masonry school building (elevation)

A preliminary elastic finite element analysis was initially performed, considering the variability in masonry strength (low to high modulus of elasticity; 2.85-5.71 GPa), soil conditions (stiff to loose; type B to D according to EN1998) and modelling approach (using shell or equivalent frame elements, Fig. 10). It was found that, in the absence of a rigid diaphragm, the modal response is strongly localised and that the long masonry panels on the plan perimeter are ineffective in resisting seismic actions transverse to their plane. Moreover, it was confirmed by comparing results from the more and less refined models, that the simpler equivalent frame model showed a modal response similar to that of its more elaborate shell-based counterpart, which renders the former a reliable, as well as practical, choice for performing the set of nonlinear analyses required for deriving fragility curves.

Several alternatives were explored for nonlinear analysis and it was finally decided to use *incremental dynamic analysis* (IDA) for the present application, since the commonly adopted for URM structures static nonlinear analysis (Kappos et al. 2002, 2006; Penelis 2006) was not applicable herein due to the absence of a prevalent mode. Moreover, the alternative scheme of modal pushover analysis was not preferred due to the existence of a large number of localized modes and the subsequent difficulties in combining the large bulk of inelastic action results in three dimensions, which could lead to unreliable results.

For the final set of nonlinear analyses, the equivalent frame model with the intermediate value of masonry strength among those considered (corresponding to E = 4.18 GPa) and stiff soil type was selected, as this also matched best the periods measured in situ. The ground was modelled by Winkler-type springs (G = 700 MPa) defined according to ASCE/SEI (2007). With respect to the pristine structure, two alternative strengthening schemes were modelled: (a) addition of a reinforced concrete band connecting the perimeter spandrels (this prevents splitting at the corners of the building and provides a small degree of diaphragm action) and (b) providing a rigid diaphragm without affecting the mass of the building (in practice this could be achieved through a steel truss at roof level).
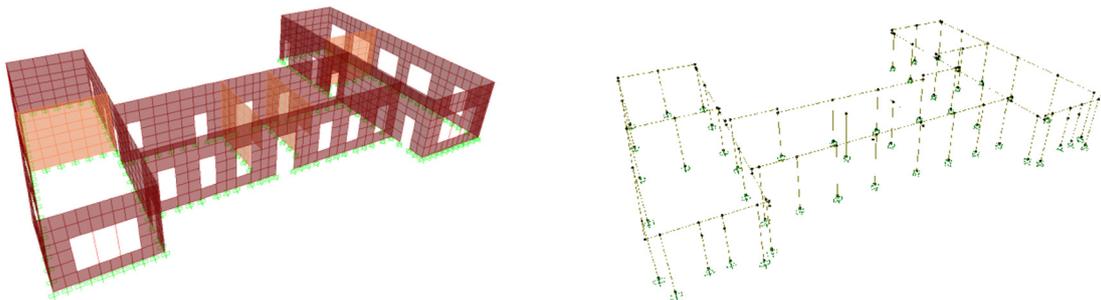

Fig. 10 Finite element modelling: shell (left) and equivalent frame

The nonlinear model properties were embedded in the form of (potential) plastic hinges on each individual frame (4 hinges for each pier, top/bottom for both directions and 2 hinges for each spandrel, acting in their strong direction). The backbone moment-rotation curves for pier hinges were calculated using the methodology suggested by Penelis (2006), which accounts for both flexure and shear. For spandrel hinges, the analytical procedure suggested by Cattari and Lagomarsino (2008) and experimentally validated by Beyer et al. (2013), was followed. The aforementioned modelling decisions resulted in a total of 180 pier and 66 spandrel hinges. For the hysteretic behaviour of the hinges, the simple kinematic model available in SAP 2000 was used.

The model loading was applied in two stages: the first step includes gravity loads (self-weight including the timber roof, and 50% of the live loading) and the second has the form of an acceleration history. Three different artificial accelerograms, compliant to Eurocode 8 (CEN 2005b) for soil type B were derived (Fig. 11), using in-house developed software (Sextos et al., 2003). For implementing the incremental dynamic analysis scheme, each record was scaled to 15 different PGA levels, from 0.01g to 1.20g. This set of analyses was repeated for both excitation directions (X and Y) and for all three different models (pristine structure, partially and fully strengthened structures). In order to fully automate the incremental dynamic analysis scheme, a custom computer program was implemented using the API interface of the employed finite element software SAP2000 (CSI 2011).
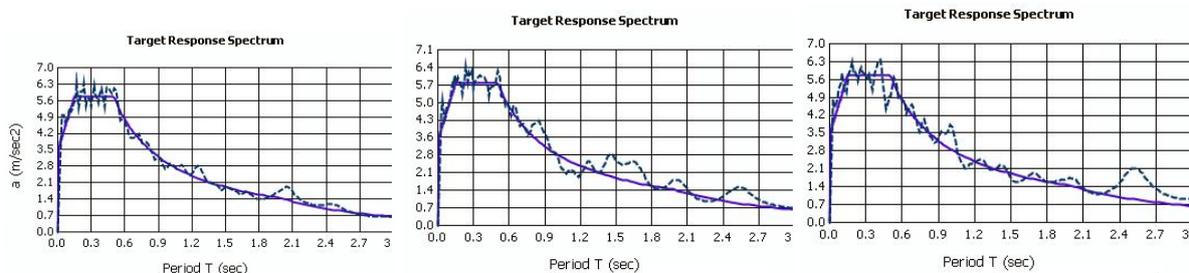

Fig. 11 Elastic response spectra of artificial accelerograms, compliant to EN1998 soil type B.

From each analysis, *local* damage indices for each equivalent frame element (piers and spandrels) were defined. Four damage states (plus the no damage state DS0) based on the maximum attained rotation in each element were specified as follows (Fig. 12):

DS0 No damage; essentially elastic response
DS1 Low damage; up to half of the rotation corresponding to residual strength
DS2 Moderate damage; up to the rotation corresponding to the threshold of residual strength
DS3 High damage; rotation corresponding to residual strength up to ultimate deformation
DS4 Collapse; strength drops to zero.

Rotation values at the threshold of DS3 and DS4 were estimated from table 7-4 of ASCE/SEI (2007). Indicative cyclic moment-rotation histories corresponding to various damage levels, taken directly from the analysis results are depicted in Fig. 13. It is noted that the kinematic hysteretic moment-rotation model employed showed satisfactory performance without numerical instabilities. Having collected the local damage indices from all (246) plastic hinges, the next step was to define the *global* damage index corresponding to each of the dynamic analyses.
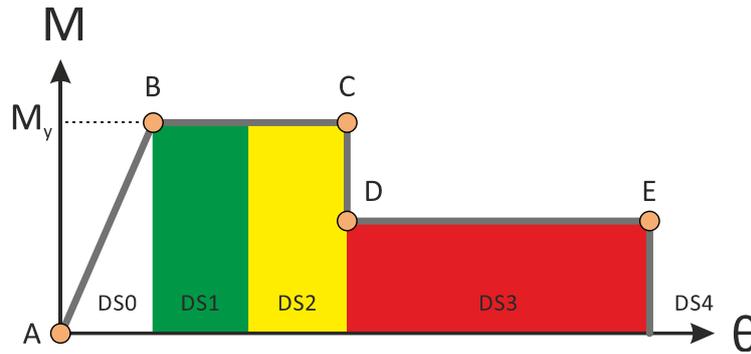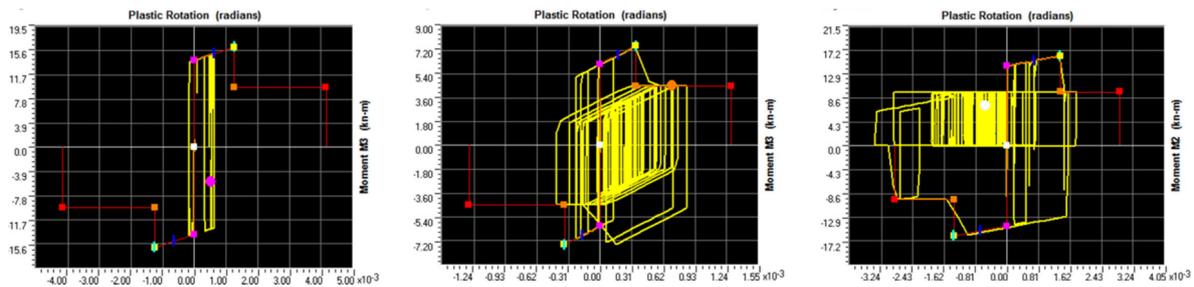
Fig. 12 Definition of damage states

Fig. 13 Cyclic moment vs. plastic rotation response for DS1, DS2 and DS4 damage levels

A rigorous evaluation of the dynamic analysis results (that showed a significant sensitivity to the adopted definition of global damage), also taking into account the recent literature on the subject (Lagomarsino & Cattari 2015), led to the definition of a lower (conservative) and an upper bound for the definition of the global damage states (limit states in Eurocode terminology, see also section 2.1), according to the following criteria:

- Lower bound (conservative): A series connection system is assumed, i.e. for assigning a global damage state of DS_x, *at least one* pier should reach a local damage state of DS_x (in one or more of its four plastic hinges). The same concept is also adopted by Lagomarsino & Cattari (2015) provided that the element is not of secondary importance. In that sense, spandrels were excluded from the definition of the global damage state.
- Upper bound (non-conservative): For assigning a global damage state of DS_x, *at least 20%* of piers should reach a local damage state DS_x (or higher). This criterion is relevant to the usual definition of structural failure, when a strength drop of about 20% takes place.

A third, intermediate, criterion was also defined for completeness, which corresponds to at least 10% of the piers reaching a local damage state DS_x (or higher). Additionally, the following criteria were implemented to derive a smooth and reasonable description of the damage evolution:

- In the case that a global damage state is skipped during the transition from one PGA level to the next (e.g. when a PGA transition from 0.5 to 0.6 yields a damage state transition from DS1 to DS3), then the intermediate PGA values corresponding to the skipped damage levels (i.e. DS2) are derived by linear interpolation.
- It was observed that at relatively high excitation levels (over 0.7 g), some dynamic analyses could not converge for the entire duration of the record (10 seconds). However, in those cases, the lower bound global damage index had already reached the collapse point (DS4) and hence the derivation of the corresponding fragility curves was not altered.

The next step was to derive the median threshold values in terms of acceleration, corresponding to each of the four different damage states (DS1 to DS4). For each of the three different models (pristine, partially and fully strengthened) and each direction (X and Y), the acceleration value corresponding to the first attainment of each damage state is calculated. Since three different acceleration records were

used, the averaged response is taken into account. Finally, the acceleration-based fragility curve for each damage state is calculated, assuming lognormal distribution, from the well-known relationship:

$$P(D > DS_x) \,|\, a = \Phi \left[\frac{1}{\beta} \cdot \ln \left(\frac{a}{a_m} \right) \right]$$

[1]

where:

$P(D>DS_x)\|$	cumulative probability for damage to reach state DS_x for a PGA equal to (a)
Φ	function of cumulative normal distribution
β	log-normal standard deviation (taken equal to 0.7 from the literature)
a	PGA value
a_m	threshold level for damage state DS_x (i.e. mean value of PGA for which the building enters DSx)

From the calculated median values for the four damage states, it was observed that no significant differences occur between the pristine and the partly strengthened model (R/C beam). However, when the full rigid diaphragm is introduced, structural damage for the same PGA level decreases significantly, particularly in the case of lower DS. It was also noted that the structure suffers lower damage across its transverse (Y) direction (due to the presence of long masonry panels) and that the upper limit criterion is not always satisfied for relatively high acceleration values. The latter issue is due to the fact that substantial damage is always localized in specific regions, leaving the rest of the elements nearly intact. In Fig. 14, an indicative damage sequence during inelastic dynamic analysis for the unstrengthened building model is depicted (PGA = 0.6 g). It is clearly seen that the plastic hinges reaching collapse (DS4; red dots) are localized in the front corner piers of the structure.
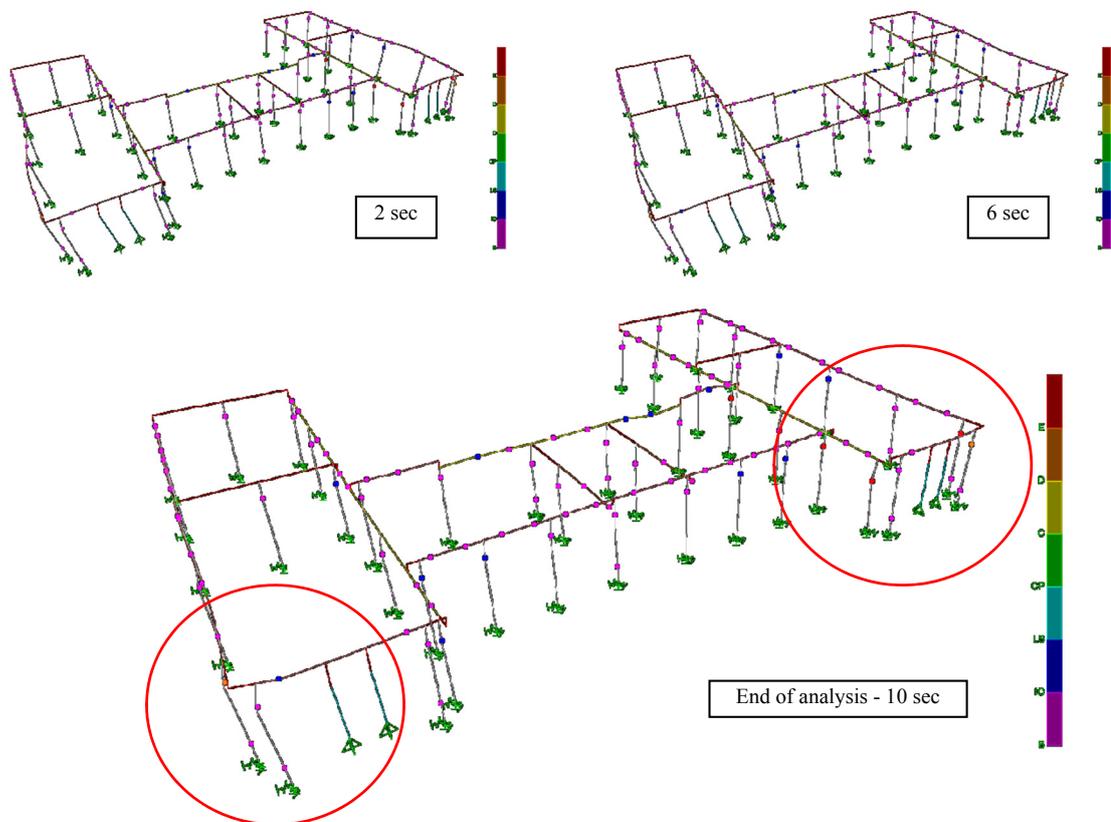

Fig. 14 Damage sequence and localisation at corners

Based on the median values and Eq. 1, the fragility curves for the pristine (original) and the rigid diaphragm building models, and for the four damage states (DS1-DS4) were plotted and are depicted in Figs. 15 and 16.
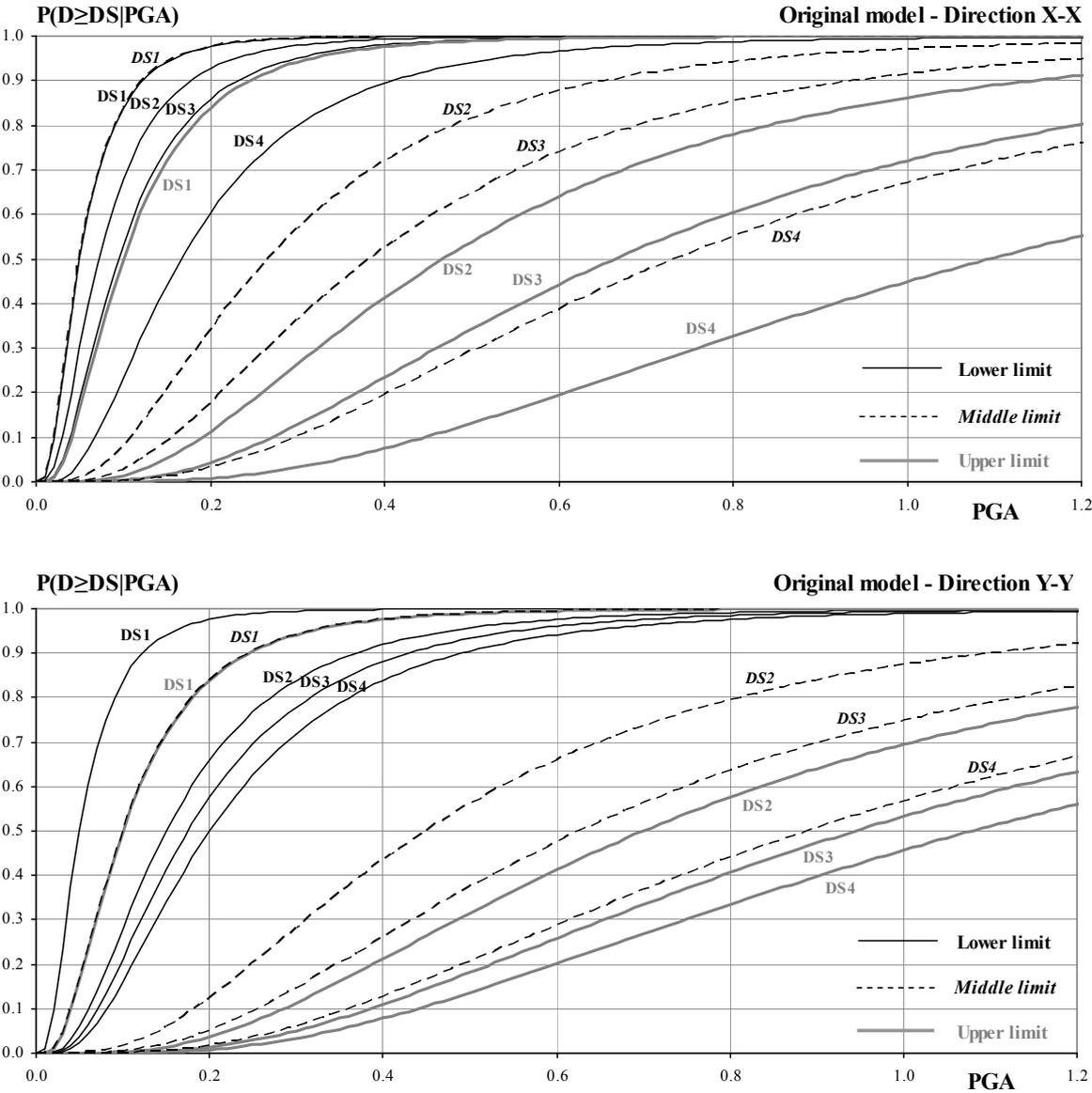

Fig. 15 Fragility curves for the pristine building model

The key point concluded from studying the derived fragility curves is the significant uncertainties emanating from the present damage state definitions. More specifically, the lower limit ('series system') seems overly conservative, whereas the upper limit leads to damage thresholds associated with very high (and arguably unrealistic) levels of seismic excitation. This is attributed to the special response characteristics of URM buildings, wherein damage is not evenly distributed along all structural elements (as in R/C structures with regular configuration) but rather localizes in certain regions. It is noted here that most of the previous similar studies (e.g. Kappos et al., 2006) are focused on planar (2D) models, where the uncertainties in the definition of damage levels are fewer compared to the present three-dimensional analysis (i.e. 2D models result in a few translational modes dominating the response, they ignore out-of plane failure, and so on).
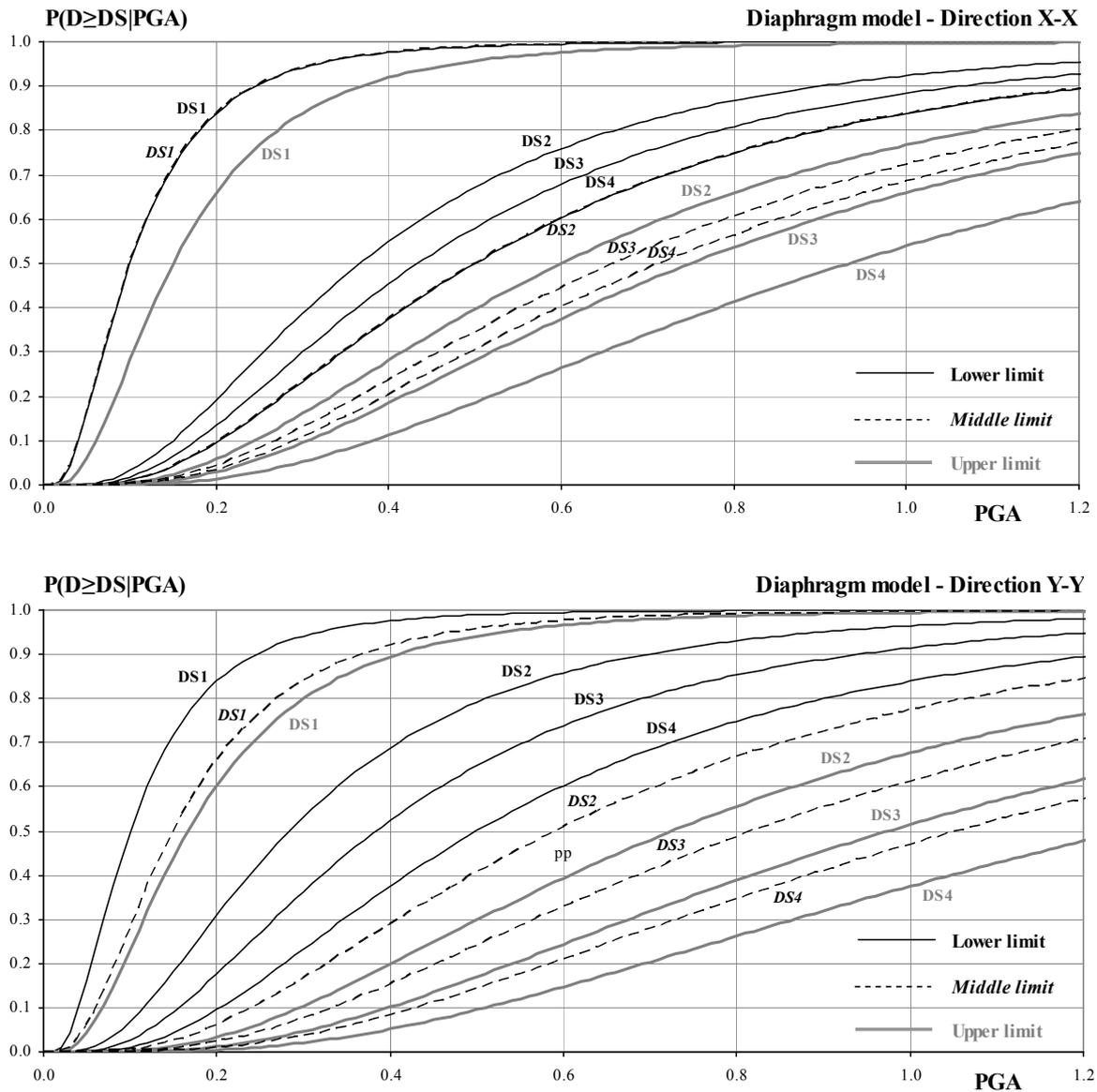
Fig. 16 Fragility curves for the fully strengthened building model (rigid diaphragm)

Finally, Table 3 gives the mean values (damage thresholds a_m) from the fragility analysis of the initial and strengthened (with the addition of an R/C band or a light rigid diaphragm) building, using the most realistic definition of global damage states ('middle limit'). It is clear from the Table that the vulnerability of the URM school buildings reduces significantly when the diaphragm retrofitting scheme is applied, but close to collapse the effect of the strengthening scheme cannot be well captured by this analysis, as numerical stability problems arise (due to several member failures).

Table 3. Thresholds a_m (g) for the URM school building in its pristine and strengthened conditions

Damage state	Pristine	With R/C band	With diaphragm
DS1	0.05	0.05	0.10
DS2	0.27	0.28	0.50
DS3	0.38	0.50	0.66
DS4	0.73	0.80	>0.72

3. Analysis of the feasibility of the strengthening programme

This section discusses the feasibility of a retrofit/strengthening programme for school buildings with the aid of cost-benefit and life-cycle cost analysis (Wen & Kang 2001a, Frangopol et al. 2001, Liu et al. 2003). Two particular questions of interest in this regard are: (i) whether a strengthening scheme is economically justified or not, and (ii) what is the optimal strengthening level. From the viewpoint of benefit-cost and life-cycle cost analysis, the potential seismic strengthening is an economic investment. As such, it is considered economically viable if the expected future benefits exceed the total cost of the investment. In this case "benefits" are the expected reduction in losses resulting (in the future) from the strengthening. Therefore, the key parameter of benefit-cost analysis is the ratio of benefit (B) to cost (C), which is determined by dividing the present value of the future benefits with the cost of carrying out (today) the strengthening. If the benefit/cost (B/C) ratio is greater than one, prospective strengthening against earthquake is economically justified. Further, if the strengthening is deemed as an investment, then the optimal retrofit/strengthening level is (by definition) the one that yields the minimum total lifetime (expected) cost.

Estimating the benefits and costs of a retrofit/strengthening programme is an inherently multidisciplinary task which involves substantial uncertainties aleatoric and/or epistemic (Ellingwood and Wen 2005, Kappos & Dimitrakopoulos 2008). The particular methodology adopted herein is that used for Greece by Kappos & Dimitrakopoulos (2008), with the following modifications:

1) The fragility curves that form the basis for calculating damage (and future losses) are those derived in the frame of this project for typical schools in Cyprus (section 2 of this paper).

2) The economic data introduced in the analysis are those for Cyprus, wherever available.

3) An ad-hoc software (COBE06) is developed (in Excel and Visual Basic platform) for calculating B/C ratios.

Fig. 17 presents the general structure of this methodology, broken down into discrete steps, and depicts the steps involving uncertainties within an ellipse.
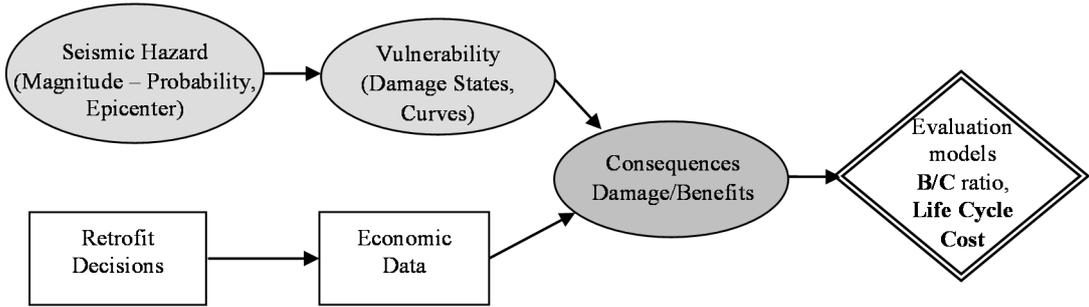

Fig. 17 Structure of the cost-benefit and life-cycle cost analysis (adapted from Kappos & Dimitrakopoulos 2008)

Herein, the same seismic hazard relationships are used as in Kappos & Dimitrakopoulos (2008), which correlate the frequency of occurrence of a seismic excitation with a given (or greater) macroseismic intensity, e.g. I_{MM} (Modified Mercalli Intensity): More specifically, equation (2), proposed by Papaioannou (2004), was first used for the Thessaloniki area after the work of Papazachos et al. (1999). Equation (3) is based on probabilistic estimation of the seismic hazard using the "FRISK88M" algorithm (Papaioannou 2004). Finally, equation (4) was used in Kappos et al. (1995) during the first benefit/cost analysis conducted in Greece and is based on calibration studies of the Greek Seismic Code.

$$\log N = 2.55 - 0.61 I_{MM} \tag{2}$$

$$\log N = 4.79 - 0.92 I_{MM} \tag{3}$$

$$\log N = 5.02 - 1.01 I_{MM} \tag{4}$$

Equation (2) yields the highest (annual) probabilities of occurrence of strong earthquakes, equation (4) the lowest, and equation (3) gives intermediate values.

3.1. Estimation of Structural Vulnerability prior and after the (potential) Strengthening

Section 2 provides fragility curves for each building type under consideration, prior to, and after, the considered strengthening schemes, similarly to Smyth et al. (2004). Thus, the vulnerability of the strengthened building is expressed through corresponding fragility curves, and the efficiency of the strengthening (R) is estimated from the decrease of the pertinent damage probabilities (e.g. $R_{Full} = D_{mv}^{LC} - D_{mv}^{HC}$) among the two fragility curves, before retrofit (D_{mv}^{LC}) and after retrofit (D_{mv}^{HC}) (Fig. 18). The D_{mv} (HC and LC) describes the structural vulnerability of the building and is the sum of the products $D_{CI,k} \cdot P_k$, where $D_{CI,k}$ is the central damage index of the kth damage state and P_k is the probability at the same damage state (Kappos and Dimitrakopoulos 2008). The fragility curves are then converted to damage probability matrices (DPMs) with the help of the empirical relationship of Koliopoulos et al. (1998) for correlating intensity I_{MM} and PGA.

$$\ln(PGA) = 0.03 + 0.74 I_{MM} \tag{5}$$

It is recalled that the efficiency of the strengthening is affected more by its ability to reduce structural damage for the frequent moderate, rather than the rare intense, earthquakes (Kappos & Dimitrakopoulos 2008).

Further, the notion of "strengthening/retrofit level" (Kappos & Dimitrakopoulos 2008) is introduced as the "intermediate" level up to which a hypothetical strengthening enhances the structural performance. Mathematically, this is expressed through the increase in the damage mean values ($D_{mv}^{Before\,R(LC)} - D_{mv}^{After\,R}$) compared to the pertinent values after full retrofit:

$$R_L = \frac{D_{mv}^{Before\,R(LC)} - D_{mv}^{After\,R}}{D_{mv}^{Before\,R(LC)} - D_{mv}^{Full\,R(HC)}} = \frac{R}{R^{Full}} \Rightarrow D_{mv}^{After\,R} = D_{mv}^{Before\,R(LC)} - R^{Full} \cdot R_L \tag{6}$$
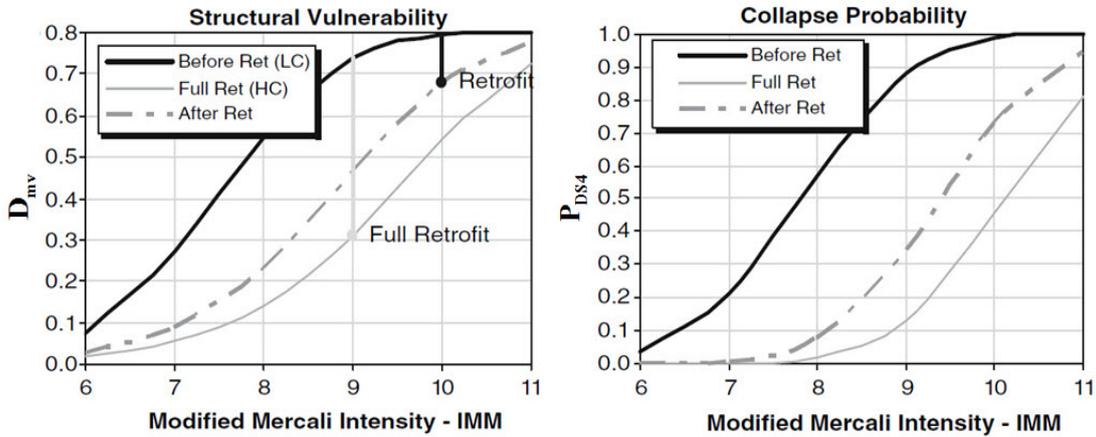

Fig. 18 Efficiency of seismic strengthening. Reduction of structural vulnerability after full or intermediate retrofit in terms of a) Mean Damage Factor (D_{MV}) and b) Collapse Probability (P_{DSi}).

Various levels of strengthening are considered herein starting from lighter and less expensive methods and going to the heaviest (and costliest) methods. Hence, the strengthening level R_L ranges from 0 (no strengthening) to 1 (full strengthening), while it could also take values greater than unity, expressing strengthening beyond the performance levels achieved with the examined schemes in section 2. For each level of strengthening the corresponding fragility curves are extrapolated from the pertinent fragility curves prior and after the strengthening.

Importantly in the case of school buildings, human life is accounted for in the estimation of benefits. To estimate the human losses (deaths and severe injuries) caused by building damage/collapse during earthquakes, the study adopts the well-known Coburn & Spence (2002) model, which correlates directly the casualties with the vulnerability of a building. The number of casualties (K_s) is given by:

$$K_S = C\left[M_1 \cdot M_2 \cdot M_3\left(M_4 + M_5\left(1 - M_4\right)\right)\right]$$ (7)

Where C is the total area of collapsed buildings; it is calculated by multiplying the area of a typical building of each category with the corresponding probability of collapse. M_1 to M5 are coefficients (Coburn and Spence 2002) related to the occupancy rate (M_1), the use of the building (M_2), the ratio of inhabitants trapped in the building due to collapse (M_3), the correlation between collapse and casualties (M_4, M_5). The pertinent values assumed in the analysis are: M_1: = 0.143 for nurseries; 0.167 for primary schools; 0.161 for secondary schools; and 0.187 for lyceums, M_2 = 0.65, M_3 = 0.30, M_4 = 0.4 and M_5 = 0.7.

3.2 Retrofit Decisions

The strengthening schemes examined in this section are the ones presented in the previous section of the paper. In summary, the strengthening methods for reinforced buildings include R/C jackets, structural walls, carbon-fibre sheets, steel elements or a mixture of the aforementioned methods (see section 2.1). For the URM buildings strengthening with R/C beams (bands) in order to provide some degree of diaphragm action to the building and provision of full diaphragm action are investigated (see section 2.2).

To assess the total retrofit cost, distinction between direct and indirect costs is made. The direct cost of the strengthening captures all expenses for materials and the rehabilitation work; it is taken as 20% of the building's replacement cost per area (i.e. €150/m^2). The indirect cost covers the engineer's fee and the cost of issuing a permit for construction works, and was taken equal to 15% of the building's replacement cost per m^2). In addition, to determine the cost of (hypothetical) intermediate-level strengthening schemes, it is assumed that the cost increases linearly from 0€/m^2 – for strengthening level = 0 (no strengthening), up to 150€/m^2 – for strengthening level = 1.

3.3 Economic Data

Regardless of the particular decision-making methodology adopted, the accuracy of the economic data is of predominant importance for the quality of the decision. Consequently, the output of the benefit-cost and the life-cycle-cost analysis presented subsequently depends heavily on the quality of the data. However, the required data is hard to acquire, at least in a form suitable for the needs of the present analysis, while on the other hand, it entails substantial uncertainties.

In general, the required economic data falls within two categories: (i) economic information specific to the examined buildings (replacement value, value of property etc.) and (ii) economic parameters of general character (discount rate, planning horizon, net present value coefficient, and statistical value of human life).

The replacement cost (R_V) is arguably the most important data item concerning buildings. It represents the cost of the replacement of the function provided by a building which must be demolished, by a new building. It is estimated as 750€/m^2 (average value for the study area at the time of the analysis). Notwithstanding ethical arguments in assigning a monetary value to human lives, the

statistical value of human life is the most significant among the parameters of general nature. Following Kappos & Dimitrakopoulos (2008), this study adopts the value of €500,000 as an upper bound emerging from the "courts awards approach" i.e. the indemnities paid in cases of death from the state or from insurance companies (FEMA 1992). Still, the uncertainties involved in the estimation of such a crucial and controversial parameter cannot be overstated.

Necessary economic parameters also include: (a) the discount rate used to convert costs (losses) due to future earthquakes into present (monetary) value. Recall that benefit/cost ratios increase as this rate decreases. The basic value considered appropriate for Cyprus is 5%. (b) The time or planning horizon of the strengthening programme (i.e. the time during which the economic benefits of the retrofit are considered). Two limit values are investigated, 20 years (lower limit) and 50 years (upper limit). (c) The "salvaged value" which is considered equal to a 20% decrease of the retrofit cost.

Table 4: Basic economic data used for calculating costs and benefits (adapted from Kappos and Dimitrakopoulos 2008).

Symbol	Cost	Equation	Basic value
C_j^{dam}	Damage of Buildings	Replacement Cost (R_V) × Floor Area × Mean Damage Factor (D_{mv})	R_V = €750/m^2 (Greece 2005)
C_j^{rel}	Relocation Expenses	Relocation cost × Gross Leasable Area × Loss of Function (time)	€7.5/m^2/month (1.0% R_V)
C_j^{loc}	Loss of Contents	Property Value × Floor Area × D_{mv}	€11.25/m^2 (5.0% R_V)
C_j^{HF}	Human fatality	Statistical Value of Human Life × Expected Deaths	€500,000 / person (upper bound)
C_j	**Total cost:**	$C_j = C_j^{dam} + C_j^{rel} + C_j^{loc} + C_j^{HF}$	

Table 4 summarizes all types of economic losses, the calculation formula, and the basic value used in the analyses presented herein for each of them. In

Table 4, index "j" indicates the losses which are calculated for macroseismic intensity j (from 6 to 11). Recall that the most critical intensities are from 6 to 8 due to their high probability of occurrence (Kappos & Dimitrakopoulos 2008).

3.4 Evaluation methods: Cost – Benefit Analysis

The next step (Fig. 17) involves the conversion of both benefits and costs into present monetary units, so the various consequences can then be summarised and evaluated. The basic assumption is that the future benefits and costs are time-invariant, constant per year (FEMA 1992). The expected annual benefits (B_0) are then calculated as:

$$B_0 = \sum_{j=VI}^{XI} N_j R_j C_j \tag{8}$$

where N_j is the expected number of earthquakes annually yielded by equations (2) to (**Error! Reference source not found.**4), R_j is the previously defined efficiency of retrofit, and C_j is the total loss (according to Table 4), all referring to seismic intensity *j*. The benefits over the planning horizon (B_t) are converted to present monetary value, according to:

$$B_t = B_0 \frac{1-(1+\lambda)^{-t}}{\lambda} \tag{9}$$

where t is the planning horizon and λ the discount rate.

The economic efficiency of a particular strengthening scheme can now be determined in terms of benefit/cost (B/C) ratios. The B/C ratio is equal to the benefits expected to accrue (due to the retrofit) over the planning period plus the cost of the deaths avoided (V_{DA}) if the cost of human life is included in the analysis, divided by the total retrofit cost (R_C) minus the salvaged value of the building (V_S), i.e. the increase in the value of the building due to the retrofit:

$$B\!/\!C = \frac{B_t + V_{DA}}{R_C - V_S} \tag{10}$$

where all four terms are expressed in present value monetary terms. The methodology, tailored to Cyprus school buildings, was implemented (utilising the in-house developed software) to carry out several B/C analyses for the different types of school buildings, including a sensitivity analysis for some key parameters like the time frame (or 'planning horizon') of the strengthening programme (20 and 50 years) and the discount rate (5%).

3.5 Evaluation methods: Life-Cycle Cost Analysis

Beyond, or regardless of, whether a potential strengthening is economically justified or not, often the question is what the optimal strengthening level is. In Life-Cycle Cost analysis terminology (Wen and Kang 2001a,b, Frangopol et al. 2001, Liu et al. 2003) the optimal strengthening level is the one that yields the minimum life-cycle cost. The total life-cycle cost is determined as the sum of the initial cost of strengthening plus the cost of the expected future losses during the lifetime of the buildings. This presupposes the calculation of the initial and lifetime costs over the time horizon of strengthening.

The lifetime total expected cost of a retrofit scheme is calculated here utilising the fragility curves derived for typical school buildings in Cyprus. The analytical expression for the total lifetime expected cost over a time horizon (t) with respect to a retrofit level R_L (the design variable) is:

$$E\big[C(t,R_L)\big] = C_0 + \bar{C} \cdot \frac{1-e^{-\lambda t}}{\lambda} \sum_{j=VI}^{XI} N_j \cdot D_{mv,j} \tag{11}$$

where, C_0 = initial cost of strengthening; $\bar{C}$ = the product of the replacement value times the floor area of the building examined; λ = discount rate/year (taken as 5%); $D_{mv,j}$ is the mean damage factor and N_j the number of earthquake occurrences per year, both for seismic intensity j and the notation E[ ] means that the cost is an expected value.

Equation (10) yields the total lifetime expected cost based on the mean damage factor. In this way, it allows a straightforward incorporation of the corresponding fragility curves, into life-cycle cost analysis. Recall that equation (10) is the simplified closed form of the total lifetime expected (Wen and Kang 2001a), valid under the assumptions that: (1) the hazard occurrences are modelled by a simple Poisson process with occurrence rate N/year, (2) the resistance is time-invariant (i.e. deterioration of structural resistance with time is ignored), (3) the structure will be restored to its original condition after each hazard occurrence, (4) the maintenance cost is negligible, and (5) $C_k = \bar{C} \cdot D_{CI,k}$ where C_k = k[th] damage - state failure cost, in present monetary value and is given by the product of the central damage index (of kth damage state -$D_{CI,k}$) times the monetary cost per loss category, resulting in:

$$\big(C_1 P_1 + C_2 P_2 + ... + C_k P_k\big) = \bar{C} \cdot D_{CI,1} \cdot P_1 + \bar{C} \cdot D_{CI,2} \cdot P_2 + ... + \bar{C} \cdot D_{CI,k} \cdot P_k = \bar{C} \cdot D_{mv} \tag{12}$$

where P_k = probability of kth damage state being reached at the time of the loading occurrence and k = total number of damage states under consideration.

3.6 Results and Discussion

This section presents the results of the benefit-cost and life-cycle-cost analyses for the strengthening of both reinforced concrete (R/C) and unreinforced masonry (URM) buildings. Four categories of building schools are considered: nurseries, primary, secondary, lyceums. In the case of the URM buildings three different sets of fragility curves are used (lower, middle and upper bound, see §2.2). Furthermore, for each building category all three seismic hazard relationships (equations (2) to (4) are examined considering two planning horizons, 20 and 50 years). Hence, 96 feasibility analyses are conducted in total.
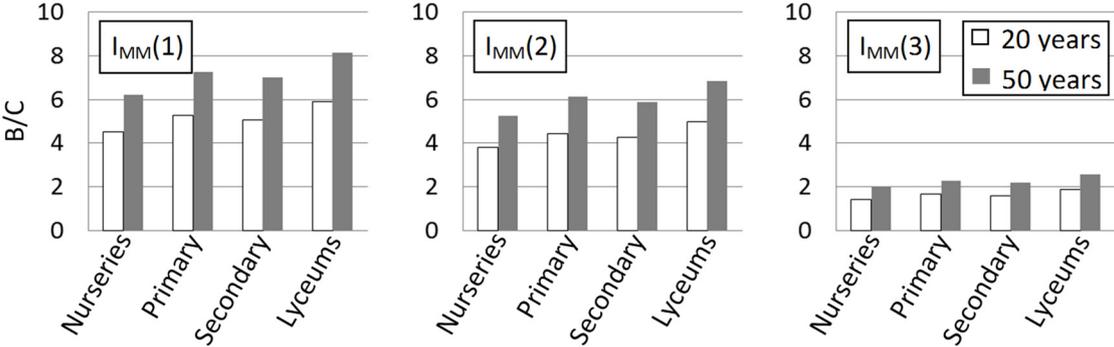

Fig. 19 Benefit/cost ratios for R/C buildings taking into account the statistical value of human life for the three hazard relationships (I_{MM} from equations 2 to 4).

Fig. 19 shows the results of a typical benefit/cost analysis for R/C school buildings based on all three hazard relationships deemed appropriate for Cyprus and accounting for the cost of human life (€500,000). It is clear that in this case retrofit of all types of schools is the appropriate choice, since B/C ratios are well above 1. Comparing the results for 20yr and of 50yr planning horizon, the B/C ratios increase for longer planning horizons, as anticipated.
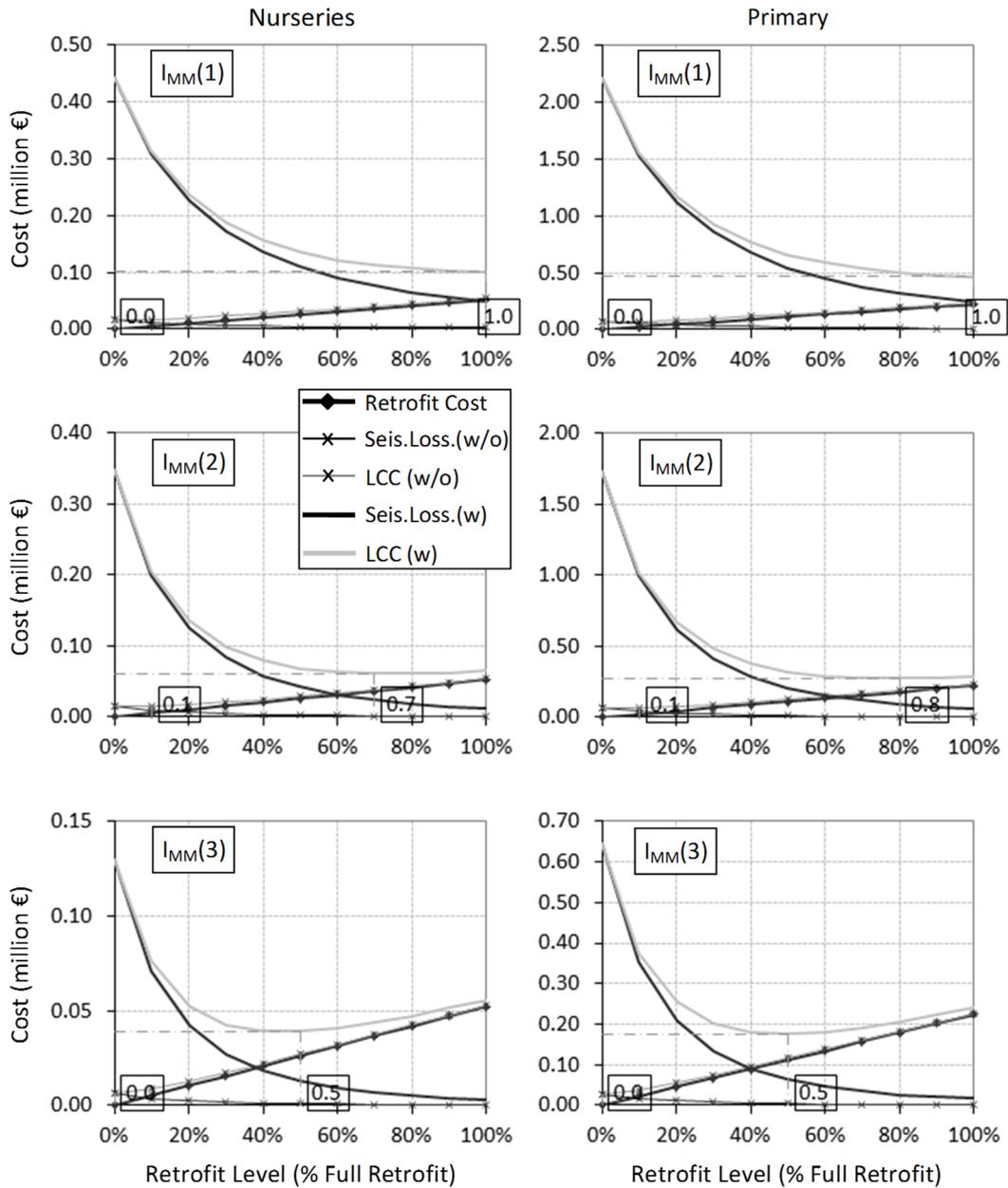
Fig. 20 Life-cycle cost analysis for reinforced concrete buildings (nurseries, primary) for the three seismic hazard relationships

Figures 20 and 21 show the results of life-cycle cost analysis for all categories of school buildings (R/C), for the cases with ("w") and without ("w/o") the cost of human life. It is seen that the optimum retrofit level is around 0.50, i.e. 50% of the cost of the heavy jacketing scheme that was described in §2.1; again, if the cost of human life is ignored, strengthening is not required. Consistently, the optimal retrofit level is higher when the seismic hazard is higher, which is expected. In the case studied, the optimal retrofit level for seismic hazard estimated according to equation (3) is lower than that for equation (2), and the lowest is found for equation (4).
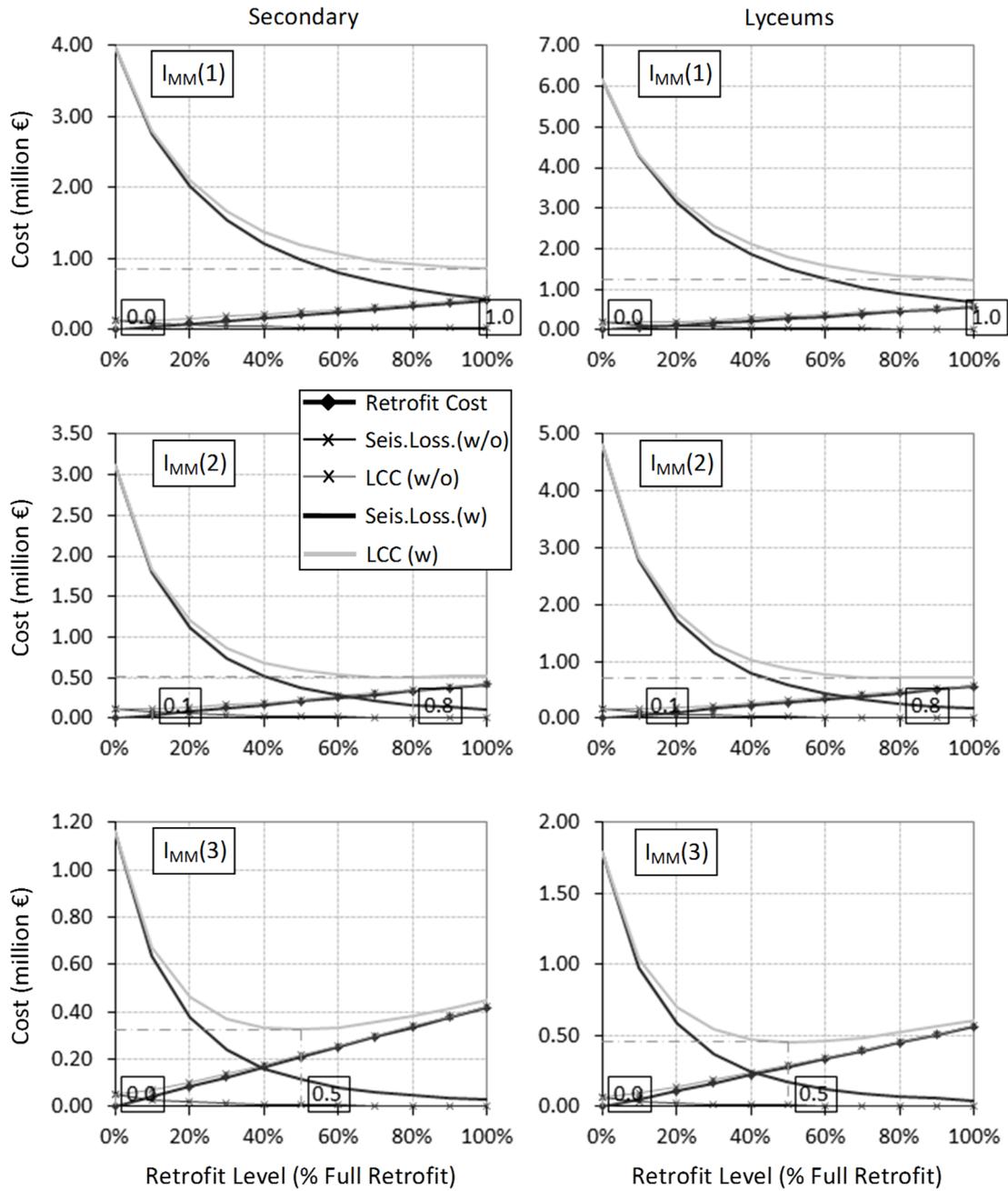
Fig. 21 Life-cycle cost analysis for R/C buildings (secondary, lyceums) for the three seismic hazard relationships

In the case of URM buildings, for all school categories and all seismic hazard relationships, when the fragility curves are based on the assumption of intermediate and upper bounds for the thresholds of damage states (see Figures 15 and 16) the optimal strengthening level is consistently zero (i.e. no strengthening); hence the pertinent plots are omitted for economy of space.
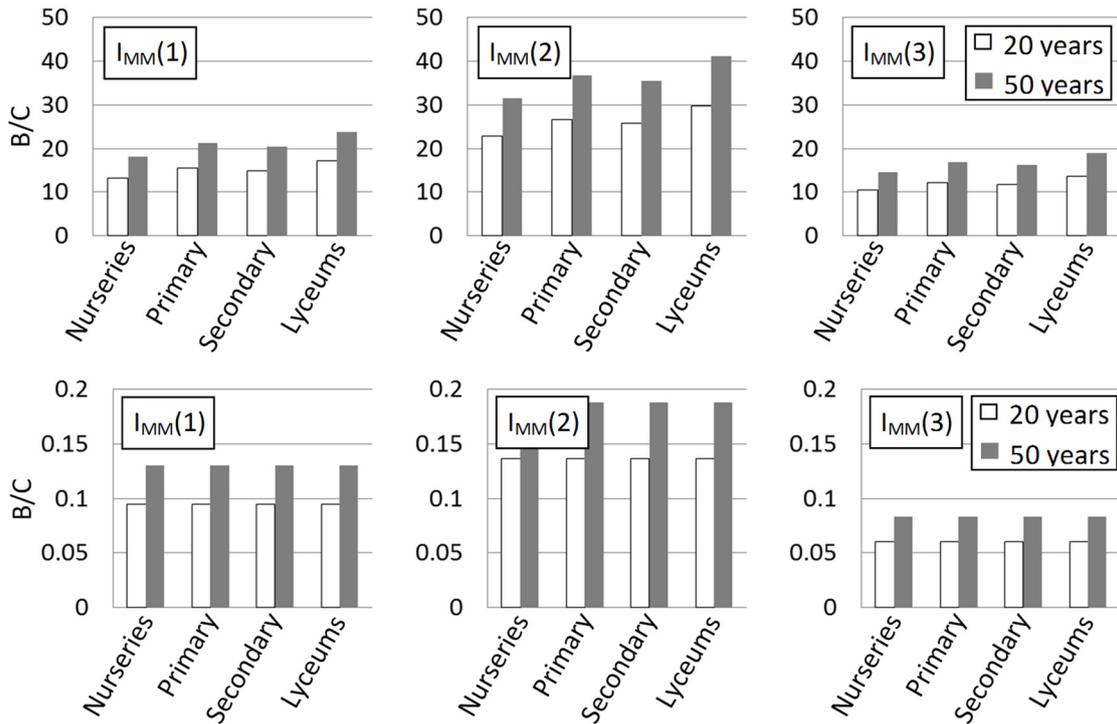
Fig. 22 Benefit/cost ratios for masonry buildings using the lower bound of fragility curves, assuming full diaphragm action after retrofit, with (top) and without (bottom) taking into account the statistical value of human life, for the three hazard relationships (I_{MM})

Fig. 22 shows the results of a typical benefit/cost analysis for URM school buildings based on all three hazard relationships including and ignoring the cost of human life. It is clear that retrofit of all types of schools is the appropriate choice only when the cost of human life is accounted for, since in this case B/C ratios are well above 1. This is due to the casualties that are expected to be avoided due to the strengthening, which are captured in monetary terms using the statistical value of human life. As a result the benefits increase and so do the B/C ratios. On the contrary, if the cost of human life is ignored in the analysis, B/C ratios are clearly below 1 and strengthening is not (economically) feasible.

As expected from the discussion presented in §2.2, for masonry buildings, the analysis was found to be very sensitive to the definition of damage states (consistently with what was mentioned previously with regard to B/C ratios); for the conservative definition of damage thresholds, i.e. the "series system". Figures 23 and 24 suggest that the recommended retrofit level is 100% (full strengthening with a rigid but light diaphragm), whereas for the least conservative definition, the recommended retrofit level is 0 (i.e. no strengthening).
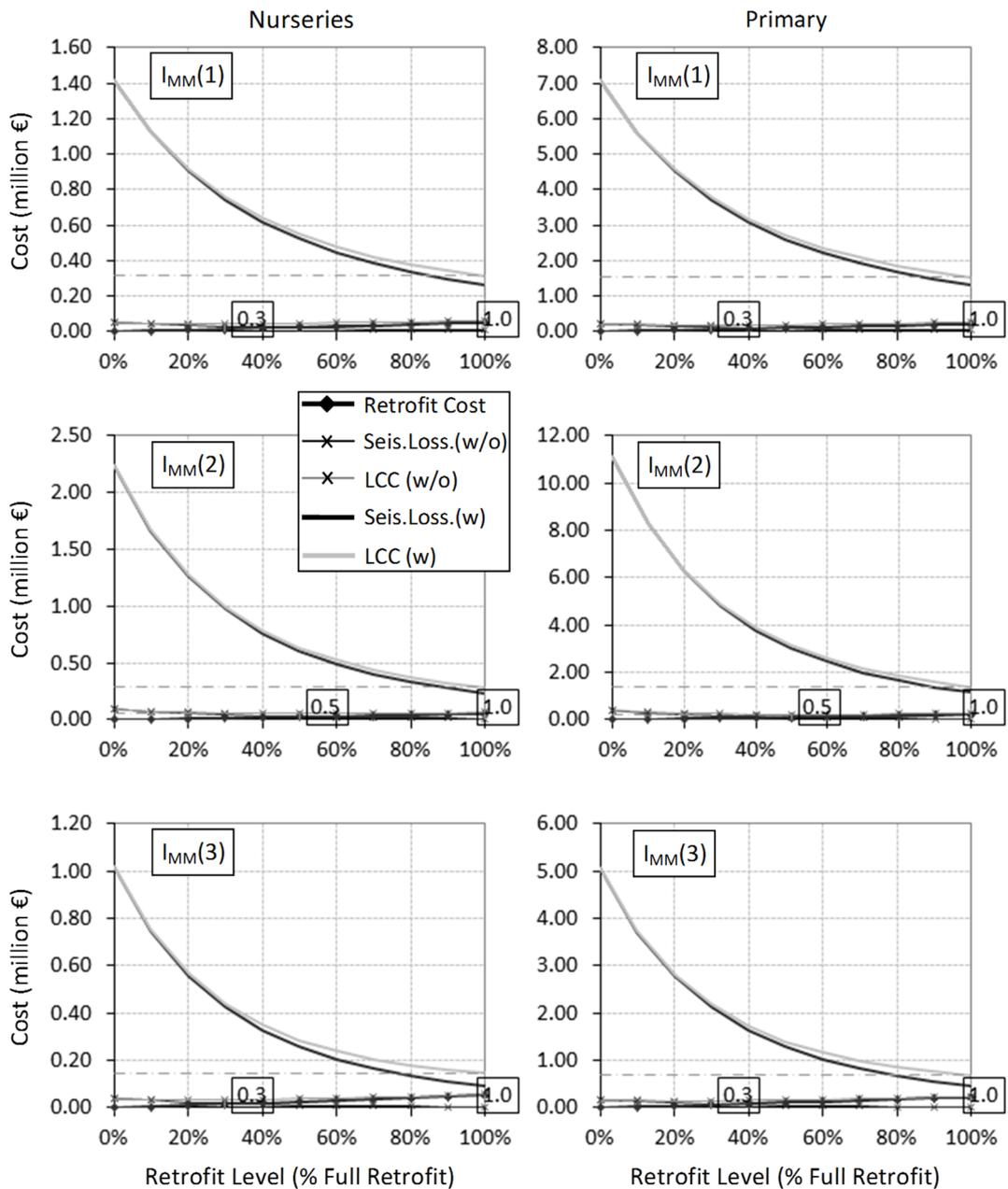
Fig. 23 Life-cycle cost analysis for unreinforced masonry buildings (nurseries, primary) for the three seismic hazard relationships

In URM schools, application of the "light" strengthening scheme (R/C band at the top) results in negligible B/C ratios (close to 0), as seen in Fig. 25; although, to a certain extent, this is due to the fact that out-of-plane failure through separation of orthogonal walls at their interconnection (a failure mode that is deemed to be prevented by continuous bands) cannot be captured in the present analysis, it is apparent that the addition of just a top band is not a satisfactory scheme. On the contrary, addition of a rigid diaphragm (e.g. steel truss), without substantially increasing the mass of the building (as would be the case if an R/C slab were added) was found to lead to B/C ratios well above 1 when human life was included in the analysis (but, again, close to 0 when neglected).
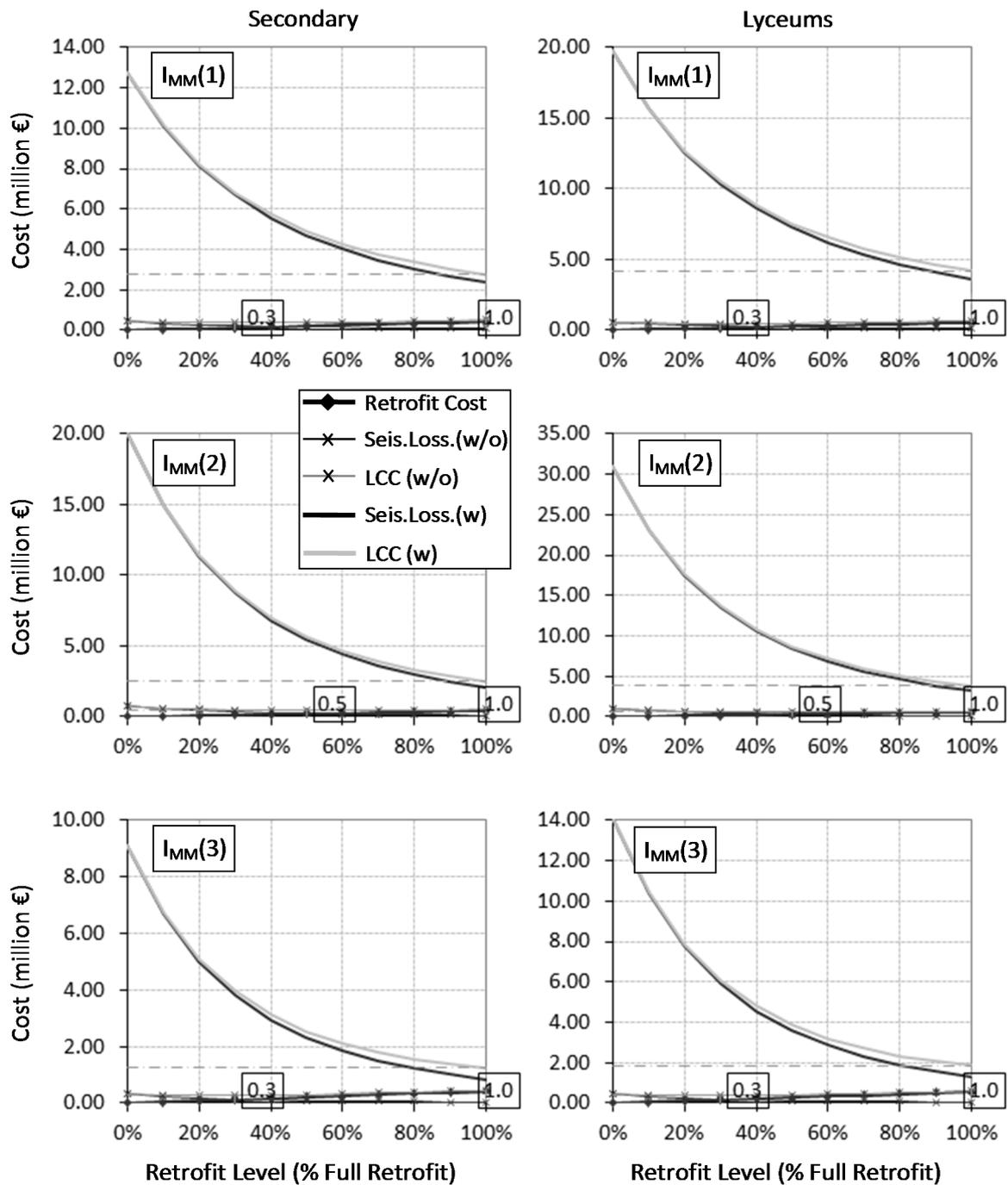
Fig. 24 Life-cycle cost analysis for unreinforced masonry buildings (secondary, lyceums) for the three seismic hazard relationships
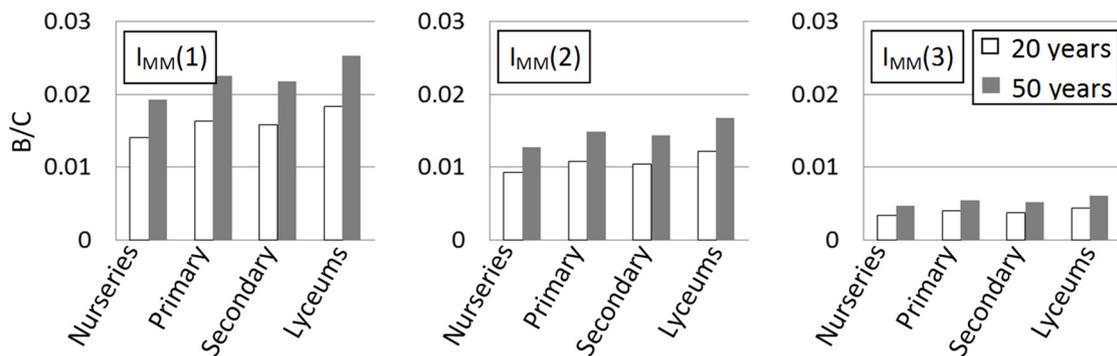
Fig. 25 Benefit/cost ratios for unreinforced masonry buildings using the upper bound of fragility curves strengthened with R/C beams (lintel) and taking into account the statistical value of human life, for the three hazard relationships (I_{MM})

4. Conclusions

The case study presented herein that deals with the unprecedented at a national level programme of strengthening school buildings in Cyprus is deemed to be of wider interest since, besides identifying strengths and weaknesses of the programme, it also reveals a number of problems associated with the application of state-of-the-art methods for seismic fragility assessment and for (economic) feasibility analysis.

One interesting finding of the first part of the study is that not all types of common buildings can be treated in a uniform way and proper decisions have to be made to not only select the most suitable methods but also to make them yield compatible results for the various types of structures addressed. In the case of reinforced concrete buildings the state-of-the-art is quite advanced and international guidelines like Eurocode 8 – Part 3 (used herein) can be adopted as a basis for defining damage states that are necessary for fragility assessment. This was not possible in the case of masonry buildings wherein a combination of relationships from the literature with values provided in the pertinent American standard (ASCE/SEI 2007) had to be duly tailored in the procedure used herein. Even the selection of inelastic analysis method (necessary for deriving fragility curves) is not equally easy in each case. In R/C buildings pushover analysis is in general possible, noting that in the case of structures with several important modes it has to be applied in its most advanced (and computationally demanding) form of multi-modal pushover. For masonry buildings without rigid diaphragms (like the school studied herein, which is by no means an exceptional case) several local modes are identified and not only application of standard pushover methods is not possible, but even multi-modal pushover is practically not feasible. Incremental dynamic analysis was adopted herein for all types of buildings studied; this is a powerful method, with a broad range of applicability, but is certainly not an easy to apply procedure. In this respect, the importance of availability of proper analysis tools cannot be overemphasised.

With regard to fragility analysis, a very sensitive issue, mostly ignored in previous studies, is the definition of global damage level in structures with a non-uniform distribution of damage, the paradigm being the (otherwise) simple masonry building without diaphragm studied herein. Several alternative criteria were explored but more work is needed in this direction, a possible direction being directly introducing the cost of repair in the definition of damage level; previous studies (e.g. Kappos et al. 2006) have shown that this approach works well (at least for R/C buildings) for the low and medium damage levels but for the other states, especially DS4, additional criteria have to be introduced.

Of equally broad interest is deemed to be the second part of the study wherein both benefit-cost and life-cycle cost analysis were applied to evaluate the effectiveness of the school strengthening programme. Some general remarks and specific conclusions derived in the course of the present study are summarised in the following:

27

- Decision making regarding pre-earthquake strengthening, is an inherently multidisciplinary task and the required data was collected from a wide variety of sources after rather strenuous efforts.

- Decisions regarding the seismic rehabilitation of existing buildings require both engineering and economic studies and consideration of social priorities.

- Valuable insight regarding retrofit benefits, as assessed from benefit-cost analysis, can be gained from the work presented herein, for instance that the feasibility of a retrofit scheme is determined more by its ability to reduce structural damage for moderate rather than strong earthquakes, at least in the common case of areas of moderate seismic hazard, as the one studied herein.

- It was seen that casualties influence benefit/cost ratios more when collapse probability is drastically reduced due to retrofit. Problems in adequately quantifying the statistical value of human life were discussed; the reference value used (€500,000) is an upper bound by the Greek standards, but is a rather conservative value for other western countries (e.g. the US). Nevertheless it amplified, in some cases up to 8 times, the benefit/cost ratios, thus shifting the outcome of the analysis towards the feasibility of retrofit. In any case, protection of life is undoubtedly the primary criterion for pre-earthquake strengthening, especially in school buildings that are studied herein.

Acknowledgements

References

Anastasiades A., Pitilakis K., Apessou M., Apostolides P., Kallioglou P., Tika T., Michaelides P., and Petrides G. Site Specific Response Analyses in Lemessos Urban Area. Proceedings 5th Hellenic Conference on Geotechnical and Geoenvironmental Engineering, Technical Chamber of Greece; 2006 (in Greek).

ASCE/SEI (2007) Seismic Rehabilitation of Existing Buildings – ASCE Standard 41-06. American Society of Civil Engineers, Reston, Virginia.

Ayyub B., and McCuen R. (1995) Chapter 4 – Simulation-based Reliability Methods in Probabilistic Structural Mechanics Handbook-Theory and Industrial Applications, Ed. Sundararajan C. R., Chapman & Hall, 53-69.

Beyer, K. and Mangalathu, S. (2013) Review of strength models for masonry spandrels, Bull. of Earthquake Engineering, 11(2): 521-542.

Cattari, S. and Lagomarsino, S. (2008) A strength criterion for the flexural behaviour of spandrels in un-reinforced masonry walls, 14th World Conference on Earthquake Engineering, Beijing, China, Paper No. 05-04-0041.

CEN (2004a) Eurocode 2: Design of Concrete Structures - Part 1: General rules and rules for buildings (EN 1992-1-1), CEN, Brussels.

CEN (2004b) Eurocode 8: Design provisions of structures for earthquake resistance - Part 1: General rules, seismic actions and rules for buildings (EN1998-1), CEN, Brussels.

CEN (2005) Eurocode 8: Design provisions of structures for earthquake resistance - Part 3: Assessment and retrofitting of buildings (EN1998-3), CEN, Brussels.

Chrysostomou, C.Z., Kyriakides, N., Kappos, A.J., Kouris L.A., Papanikolaou, V., Georgiou, E. and Millis, M. (2013) Seismic Retrofitting and Health Monitoring of School Buildings of Cyprus. The Open Construction and Building Technology Journal, 7: 208-220.

Coburn A. and Spence R., (2002) Earthquake Protection, Second Edition, John Wiley & Sons Ltd., Chichester, England.

CSI [Computers & Structures Inc.] (2011) SAP2000 – Version 15.0.1 : Linear and Non linear Static and Dynamic Analysis and Design of Three-Dimensional Structures, Berkeley, California.

Ellingwood B.R., & Wen Y.K., (2005): Risk–benefit-based design decisions for low- probability/high consequence earthquake events in Mid-America. Prog. Struct. Engng Mater., 7: 56–70

FEMA (1992) A Benefit Cost - Model for the Seismic Rehabilitation of Structures", Volumes 1,2.

FEMA-NIBS (2003) Multi-hazard Loss Estimation Methodology - Earthquake Model: HAZUS®MH Technical Manual, Washington DC.

Frangopol D.M., Kong J.S., and Gharaibeh E.S. (2001) Reliability-Based Life-Cycle Management of Highway Bridges. Journal of Computing in Civil Engineering, 15(1): 27-34

Japan Ministry of Education, Culture, Sports, Science and Technology (2006) Seismic Retrofitting Quick Reference - School Facilities that Withstand Earthquakes, Tokyo.

Kappos A.J. and Dimitrakopoulos E.G. (2008) Feasibility of pre-earthquake strengthening of buildings based on cost-benefit and life-cycle cost analysis, with the aid of fragility curves. Nat. Hazards, 45(1): 33-54.

Kappos, A.J., Panagopoulos, G., Panagiotopoulos, C. and Penelis, G. (2006) A hybrid method for the vulnerability assessment of R/C and URM buildings. Bull. of Earthquake Engineering 4(4): 391-413.

Kappos A.J., Penelis, Gr.G., and Drakopoulos, C. (2002) Evaluation of simplified models for the analysis of unreinforced masonry (URM) buildings. Journal of Structural Engineering, ASCE, 128(7): 890-897.

Kappos A. J., Pitilakis K., Stylianidis K., Morfidis K., Asimakopoulos D. (1995) Cost-Benefit Analysis for the Seismic Rehabilitation of buildings based on a hybrid method of Vulnerability Assessment, 3rd International Conference on Seismic Zonation, Vol I, Nice, France, 406-413.

Koliopoulos P.K., Margaris B.N., & Klimis N.S. (1998) Duration and energy characteristics of Greek strong motion records. Journal of Earthquake Engineering, 2(3): 391-417.

Kyriakides N., Ahmad S., Pilakoutas K., Neocleous K., and Chrysostomou C. (2014) A Probabilistic Analytical Seismic Vulnerability Assessment Framework for Low Strength Structures of Developing Countries. Earthq. and Structures; 6,(6): 665-87. http://dx.doi.org/10.12989/eas.2014.6.6.665.

Lagomarsino, S. and Cattari, S. (2015) PERPETUATE guidelines for seismic performance-based assessment of cultural heritage masonry structures, Bull. of Earthq. Engng, 13(1), , 13–47.

Liu M., Burns S.A., & Wen Y.K. (2003) Optimal seismic design of steel frame buildings based on life-cycle cost considerations", Earthquake Engineering & Structural Dynamics, 32: 1313–1332 .

McKay M., Conover W., and Beckman R. (1979) A comparison of three methods for selecting values of input variables in the analysis of output from a computer code. Technometrics, 21: 239-245.

OECD (2004) Keeping Schools Safe in Earthquakes; a publication of the OECD Programme on Educational Building (PEB).

Papaioannou C. A., (2004) *Seismic Hazard Scenarios – Probabilistic Assessment of the Seismic Hazard Report for WP 02 of the project SRM-LIFE* (scientist in charge K. Pitilakis), ITSAK, Thessaloniki (in Greek)

Papazachos B. C., Savaidis A. A., Papaioannou C. A., Papazachos C.B (1999) The S. Balkan Bank of shallow and intermediate depth earthquake microseismic data, XXII Gen. Ass. Of the IUGG, Birmingham, UK, July 1999 (abstracts volume)

Penelis, G. G. (2006) An Efficient Approach for Pushover Analysis of Unreinforced Masonry (URM) Structures". Journal of Earthquake Engineering, 10(3): 359–379.

Sextos A.G., Pitilakis K.D., and Kappos A.J. (2003) Inelastic dynamic analysis of R/C bridges accounting for spatial variability of ground motion, site effects and soil-structure interaction phenomena. Part 1: Methodology and analytical tools. Earthquake Engineering & Structural Dynamics, 32(4): 607–627.

Smyth A. W., Altay G. I., Deodatis G., Erdik M., Franco G., Gulkan P., Kunreuther H., Lus H., Mete E., Seeber N., and Yuzugullu O. (2004) Probabilistic Benefit/cost Analysis for Earthquake Damage Mitigation: Evaluating Measures for Apartment Houses in Turkey. Earthq Spectra, 20(1): 171–203.

Ventura, C.E., Finn, W.D.L., Bebamzadeh A., Pina F. and Taylor, G.W. (2012) Seismic Retrofit of School Buildings in British Columbia, Canada, Proceed. 12th World Conf. on Earthquake Engineering, Lisbon, paper no. 5496.

Wen Y. K., Kang Y. J. (2001a) Minimum Building Life-Cycle Cost Design Criteria. I: Methodology. Journal of Structural Engineering, ASCE, 127(3): 330-337.

Wen Y.K., & Kang Y.J., (2001b) Minimum Building Life-Cycle Cost Design Criteria. II: Applications. Journal of Structural Engineering, 127(3): 338-346.